Engineering heterologous molybdenum-cofactor-biosynthesis and nitrate-assimilation pathways enables nitrate utilization by Saccharomyces cerevisiae

Perli, Thomas; van der Vorm, Daan N.A.; Wassink, Mats; van den Broek, Marcel; Pronk, Jack T.; Daran, Jean Marc

DOI
10.1016/j.ymben.2021.02.004

Publication date
2021

Document Version
Final published version

Published in
Metabolic Engineering

Metabolic Engineering 65 (2021) 11–29

Contents lists available at ScienceDirect

Metabolic Engineering

journal homepage: www.elsevier.com/locate/meteng

Engineering heterologous molybdenum-cofactor-biosynthesis and nitrate-assimilation pathways enables nitrate utilization by *Saccharomyces cerevisiae*

Thomas Perli, Daan N.A. van der Vorm, Mats Wassink, Marcel van den Broek, Jack T. Pronk, Jean-Marc Daran *

Department of Biotechnology, Delft University of Technology, Van der Maasweg 9, 2629, HZ, Delft, the Netherlands

ARTICLE INFO

Keywords:
Molybdenum cofactor
Nitrate reductase
Nitrate assimilation
Saccharomyces cerevisiae
Metabolic engineering

ABSTRACT

Metabolic capabilities of cells are not only defined by their repertoire of enzymes and metabolites, but also by availability of enzyme cofactors. The molybdenum cofactor (Moco) is widespread among eukaryotes but absent from the industrial yeast *Saccharomyces cerevisiae*. No less than 50 Moco-dependent enzymes covering over 30 catalytic activities have been described to date, introduction of a functional Moco synthesis pathway offers interesting options to further broaden the biocatalytic repertoire of *S. cerevisiae*. In this study, we identified seven Moco biosynthesis genes in the non-conventional yeast *Ogataea parapolymorpha* by *Spy*Cas9-mediated mutational analysis and expressed them in *S. cerevisiae*. Functionality of the heterologously expressed Moco biosynthesis pathway in *S. cerevisiae* was assessed by co-expressing *O. parapolymorpha* nitrate-assimilation enzymes, including the Moco-dependent nitrate reductase. Following two-weeks of incubation, growth of the engineered *S. cerevisiae* strain was observed on nitrate as sole nitrogen source. Relative to the rationally engineered strain, the evolved derivatives showed increased copy numbers of the heterologous genes, increased levels of the encoded proteins and a 5-fold higher nitrate-reductase activity in cell extracts. Growth at nM molybdate concentrations was enabled by co-expression of a *Chlamydomonas reinhardtii* high-affinity molybdate transporter. In serial batch cultures on nitrate-containing medium, a non-engineered *S. cerevisiae* strain was rapidly outcompeted by the spoilage yeast *Brettanomyces bruxellensis*. In contrast, an engineered and evolved nitrate-assimilating *S. cerevisiae* strain persisted during 35 generations of co-cultivation. This result indicates that the ability of engineered strains to use nitrate may be applicable to improve competitiveness of baker's yeast in industrial processes upon contamination with spoilage yeasts.

1. Introduction

Catalytic activities of many enzymes strictly depend on cofactors, which comprise a chemically diverse collection of non-protein organic compounds (coenzymes) and metal ions (Alberts, 2018; Broderick, 2001; Champe et al., 2005). In wild-type micro-organisms, cofactor requirements can strongly influence their catalytic capabilities and/or nutritional requirements. Many vitamins, which are essential organic molecules that cannot be synthesized by the organism itself and therefore have to be supplemented to growth media (Combs Jr and McClung, 2016), are in fact cofactors or precursors of them. For example, in the yeast *Saccharomyces cerevisiae*, the vitamin biotin is an essential cofactor for three carboxylases (pyruvate carboxylase Pyc1 and Pyc2, urea carboxylase Dur1,2 or acetyl-CoA carboxylase Acc 1) and can be taken up from growth media by the native biotin transporter Vht1 (Perli et al., 2020c; Stolz et al., 1999). *S. cerevisiae* strains belonging to the widely used S288c lineage completely lack two genes (*BIO1* and *BIO6*) required for synthesis of biotin, while many other strains of this industrially relevant yeast grow poorly in biotin-free media (Bracher et al., 2017; Burkholder et al., 1944; Phalip et al., 1999; Wu et al., 2005).

When the enzyme repertoire of cells is expanded by metabolic engineering, new cofactor requirements can be introduced. However, nutritional supplementation of these new requirements in culture media may not always be possible due to either lack of supply, high costs and/

* Corresponding author.
E-mail addresses: t.perli@tudelft.nl (T. Perli), D.N.A.vanderVorm@student.tudelft.nl (D.N.A. van der Vorm), M.Wassink-1@student.tudelft.nl (M. Wassink), Marcel.vandenBroek@tudelft.nl (M. van den Broek), j.t.pronk@tudelft.nl (J.T. Pronk), j.g.daran@tudelft.nl (J.-M. Daran).

https://doi.org/10.1016/j.ymben.2021.02.004
Received 9 November 2020; Received in revised form 28 January 2021; Accepted 15 February 2021
Available online 20 February 2021

or absence of membrane transporters for such compounds. In such cases, strain design should include introduction of heterologous cofactor uptake systems and/or pathways for *de novo* cofactor biosynthesis. For example, since *S. cerevisiae* lacks Ni-dependent enzymes and a Ni transporter, replacement of its ATP-dependent urease (Dur1,2) by a heterologous nickel-dependent, ATP-independent enzyme required co-expression of a Ni transporter (Milne et al., 2015). Expansion of the organic cofactor repertoire of *S. cerevisiae* is exemplified by studies on *de novo* biosynthesis of opioids in this yeast, which required biosynthesis of tetrahydrobiopterin, the cofactor of the tyrosine hydroxylase that catalyses the first committed step of the (S)-reticuline pathway (Galanie et al., 2015; Li and Smolke, 2016).

The transition metal molybdenum (Mo, typically bioavailable as molybdate MoO_4^{2-}) is an essential trace element for many organisms across the three domains of life. Molybdate is typically incorporated in a tricyclic pterin-based scaffold called molybdopterin to form a molybdenum cofactor (Moco). With the notable exception of nitrogenases, which contain an Fe–Mo-cofactor, all known molybdoenzymes harbour

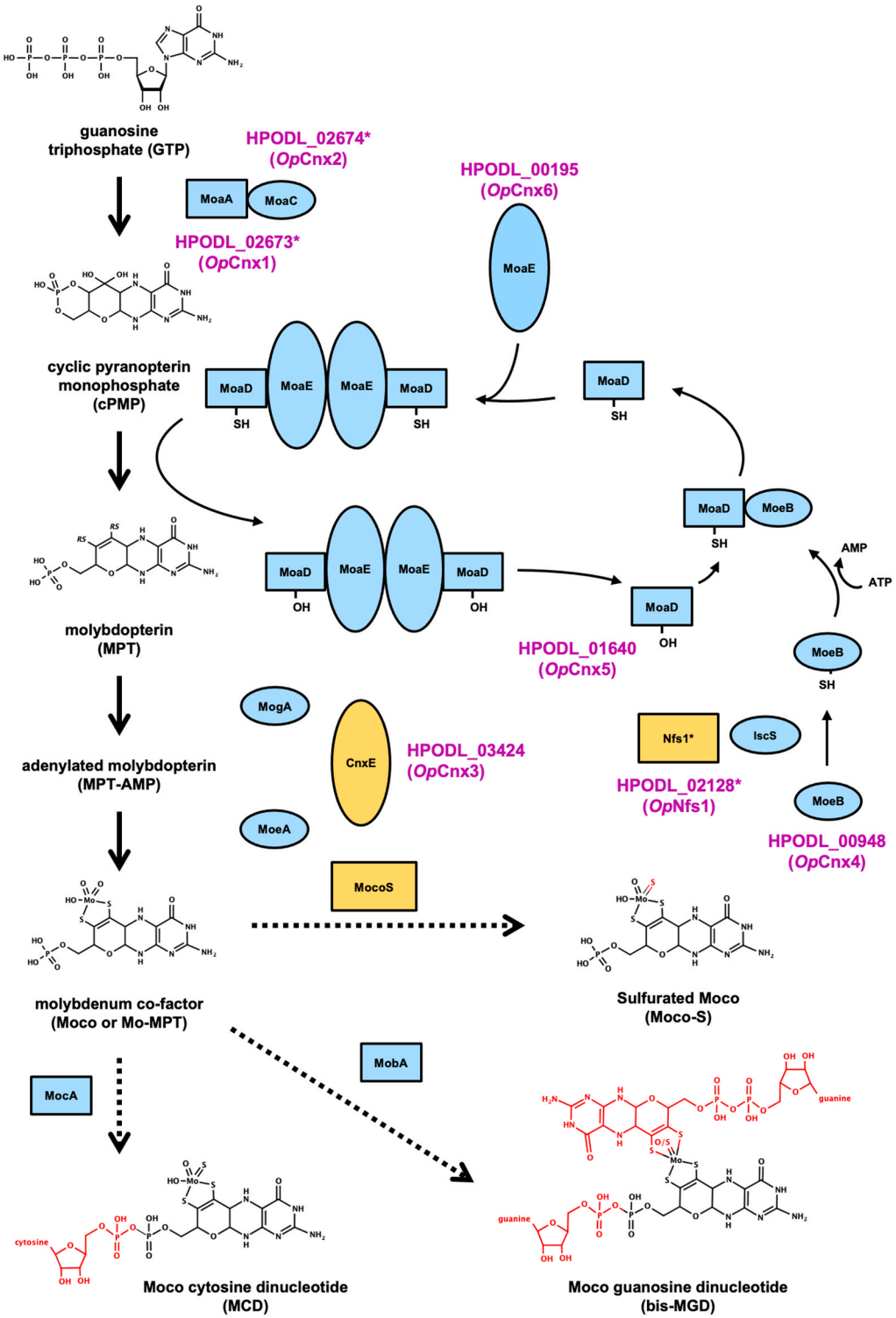

Fig. 1. Schematic representation of the molybdenum-cofactor biosynthesis pathway. GTP is first converted to cPMP by the heterodimer MoaA/MoaC, this step takes place in the mitochondria in eukaryotic cells. Then, MoaD transfers its sulfur moiety to cPMP to yield MPT. MoaD is recycled by sulfur transfer from MoeB, which is itself sulfurated by IscS. MPT is then first adenylated after which the MoO_4^{2-} oxyanion is inserted by the heterodimer MogA/MoeA. In eukaryotes, the latter reaction is catalysed by a single protein (Gephyrin). Moco can be sulfurated at the Mo site by a Moco sulfurase (MocoS) to form sulfurated Moco (Moco-S). Moreover, Moco can be further modified in prokaryotic cells by addition of either cytosine (MocA) or guanosine (MobA) to form Mo-molybdopterin cytosine dinucleotide (MCD) and bis(molybdopterin guanine dinucleotide)molybdenum (bis-MGD), respectively. *E. coli* proteins, fungal homologs, *O. parapolymorpha* homologs and Moco modifications are shown in light blue, yellow, magenta, and red, respectively. Mitochondrial proteins are indicated by an asterisk.

Moco variants in their active sites (Rajagopalan and Johnson, 1992; Rubio and Ludden, 2008; Schwarz et al., 2009). Moco biosynthesis is conserved and extensively studied in prokaryotes and eukaryotes (Iobbi-Nivol and Leimkuhler, 2013; Mendel, 2013; Rajagopalan and Johnson, 1992). Nitrate-assimilating yeasts such as *Ogataea parapolymorpha* and *Brettanomyces bruxellensis* synthesize a Moco that is required for activity of nitrate reductase (Linder, 2019). In contrast, the industrial yeast and eukaryotic model *S. cerevisiae* is devoid of Mo-dependent enzymes and cannot synthesize Moco nor assimilate nitrate (Peng et al., 2018; Zhang et al., 2011).

In eukaryotes, the first step of Moco synthesis (Fig. 1), which converts GTP onto cyclic pyranopterin monophosphate (cPMP), takes place in mitochondria. After export of cPMP to the cytosol, it is first sulfurated to form molybdopterin (MPT). The MPT synthase that catalyses this sulfuration is then regenerated by a sulfur mobilization route involving the FeS-cluster protein IscS (Nfs1 in eukaryotes), which is shared with the tRNA thiolation pathway (Leimkuhler et al., 2017). Finally, MPT is adenylated to form MPT-AMP and, after hydrolysis of the adenylate group, molybdate is inserted into the MPT dithiolene group to form the Moco Mo-MPT (Iobbi-Nivol and Leimkuhler, 2013). Mo-MPT can be further modified in prokaryotes by addition of either cytosine or guanosine to form the Moco variants MPT-cytosine dinucleotide (MCD) or MPT-guanine dinucleotide (MGD), respectively. Prokaryotes as well as eukaryotes can further modify Moco variants by replacing one oxo ligand on the Mo atom by a sulfido ligand to form the mono-oxo Moco variant (Moco-S).

Molybdoenzymes typically use the versatile redox chemistry of MoO_4^{2-} to catalyse redox reactions, often involving oxygen transfer (Hille, 2002). Based on the ligands at the Mo atom of their Moco, molybdoenzymes are divided in three families: the xanthine oxidase (XO) family, the sulfite oxidase (SO) family and the dimethyl sulfoxide reductase (DMSOR) family (Hille et al., 2014). The XO family requires MCD or Moco-S at the catalytic site while the SO family contains Mo-MPT. Members of the DMSOR family instead require the bis-MGD cofactor, which is formed from MoMPT by first forming a bis-Mo-MPT intermediate followed by addition of GMP moieties to its two C-4 phosphates (Lake et al., 2000; Palmer et al., 1996). Recently, bis-Mo-MPT itself has been shown to act as cofactor for the *Escherichia coli* oxidoreductase YdhV (Reschke et al., 2019). To date, over 50 Mo-containing enzymes have been purified and characterized while many genes have been predicted to encode additional, as yet uncharacterized molybdoproteins (Cvetkovic et al., 2010; Hille et al., 2014).

Its excellent accessibility to genome editing and availability of cost-effective procedures for large-scale industrial fermentation have made *S. cerevisiae* a popular platform for production non-native low-molecular weight compounds (Nielsen, 2019; Ostergaard et al., 2000). Introduction of a functional Moco biosynthesis pathway into *S. cerevisiae* would constitute an important step towards further expansion of the versatility of this yeast as a metabolic engineering platform, for example by enabling the expression of industrially relevant molybdoproteins such as nitrate reductase and/or metal-dependent formate dehydrogenases. A nitrate-assimilating *S. cerevisiae* strain could increase the robustness of industrial biotechnology processes relying on nitrate containing feedstocks. Nitrate is for instance, often found in sugarcane juice and nitrate levels have been shown to correlate with the fraction of spoilage yeast *B. bruxellensis* found in the fermented must. The inability of *S. cerevisiae* to utilize this nitrogen source has been considered as a critical factor for *B. bruxellensis* contamination in Brazilian ethanol plants (da Silva et al., 2016; de Barros Pita et al., 2011).

To explore introduction of Moco biosynthesis in *S. cerevisiae*, we first functionally analysed structural genes involved in this process in the nitrate-assimilating yeast *O. parapolymorpha* by Cas9-mediated mutational analysis (Juergens et al., 2018; Winzeler et al., 1998). The identified *O. parapolymorpha* genes were expressed in *S. cerevisiae*. To enable *in vivo* analysis of the functionality of the heterologous Moco pathway, we co-expressed the *O. parapolymorpha* nitrate assimilation pathway, which includes a Moco-dependent nitrate reductase. As *S. cerevisiae* is not known to harbour a specific molybdate transporter (Tejada-Jimenez et al., 2007), a high-affinity molybdate transporter from *Chlamydomonas reinhardtii* (*Cr*Mot1) was also included in strain designs. Aerobic and anaerobic cultures of engineered *S. cerevisiae* strains were tested and evolved in the laboratory for the ability to use nitrate as sole nitrogen source, followed by whole-genome sequencing of evolved strains to identify relevant mutations. In addition, co-consumption of nitrate and ammonium, as well as the ability to assimilate nitrate at nM concentrations of molybdate were investigated. A possible industrial advantage of nitrate-assimilating *S. cerevisiae* was investigated in co-cultivation experiments with the nitrate-assimilating spoilage yeast *B. bruxellensis*.

2. Material and methods

2.1. Strains, media and maintenance

Yeast strains used and constructed in this study are shown in Table 1. *O. parapolymorpha* strains were derived from the DL-1 strain (Ravin et al., 2013). *B. bruxellensis* strain CBS 2499 (Smith et al., 1990) was obtained from the Westerdijk Institute (Utrecht, The Netherlands). All *S. cerevisiae* strains were derived from the CEN. PK lineage (Entian and Kötter, 2007; Salazar et al., 2017). Yeast strains were grown on either YP (10 g/L Bacto yeast extract, 20 g/L Bacto peptone) or SM medium (Verduyn et al., 1992) with either 5 g/L KNO_3, 5 g/L $(NH_4)_2SO_4$, 0.6 g/L acetamide, 0.8 g/L NH_4NO_3, or 2.3 g/L urea (SM_{NO3}, SM_{Amm}, SM_{Ac}, SM_{AN}, and SM_{urea}, respectively) as sole nitrogen source. For *O. parapolymorpha* cultures grown on SMD_{NO3}, KNO_3 was substituted with 4.25 g/L $NaNO_3$. In all SM media variants, with the exception of SM_{Amm}, 6.6 g/L K_2SO_4 was added as a source of sulfate (Solis-Escalante et al., 2013). YP or SM media were autoclaved at 121 °C for 20 min prior to addition of 1 mL/L of filter-sterilized vitamin solution (Verduyn et al., 1992). For anaerobic growth experiments, sterile media were supplemented with Tween 80 (polyethylene glycol sorbate monooleate, Merck, Darmstadt, Germany) and ergosterol (≥95% pure, Sigma-Aldrich, St. Louis, MO) as described previously (Dekker et al., 2019). A concentrated glucose solution was autoclaved at 110 °C for 20 min and then added to the YP and SM medium at a final concentration of 20 g/L, yielding SMD and YPD, respectively. For testing the essentiality of a heterologously expressed high-affinity molybdenum transporter, the Mo concentration in the medium was lowered from 1.6 μM to 16 nM, yielding $SMD_{NO3-LowMo}$. 500-mL Shake flasks containing 100 mL medium and 100-mL shake flasks containing 20 mL medium were incubated at 30 °C and 200 rpm in an Innova Incubator (Brunswick Scientific, Edison, NJ). Solid media were prepared by adding 1.5% (w/v) Bacto agar and, where indicated, 200 mg/L G418 or 200 mg/L hygromycin. *Escherichia coli* strains were grown in LB (10 g/L Bacto tryptone, 5 g/L Bacto yeast extract, 5 g/L NaCl) supplemented with 100 mg/L ampicillin or kanamycin. To discriminate between *S. cerevisiae* and *B. bruxellensis* in competition experiments (Jespersen and Jakobsen, 1996), filter-sterilized bromocresol green (Sigma-Aldrich) at a final concentration of 88 mg/L was added to either SMD_{NO3} or SMD_{Amm} agar medium ($SMD_{NO3\text{-}blue}$ and $SMD_{Amm\text{-}blue}$, respectively). *S. cerevisiae* and *E. coli* cultures were stored at −80 °C after the addition of 30% v/v glycerol.

2.2. Molecular biology techniques

Primers used in this study are shown in Table 2. DNA was amplified using Phusion Hot Start II High Fidelity Polymerase (Thermo Scientific, Waltham, MA) and desalted or PAGE-purified oligonucleotide primers (Sigma-Aldrich) according to manufacturers' instructions. Diagnostic PCR reactions were performed with DreamTaq polymerase (Thermo Scientific). PCR products were separated by gel electrophoresis on a 1% (w/v) agarose gel (Thermo Scientific) in TAE buffer (40 mM Tris, 20 mM acetic acid, 1 mM EDTA; Thermo Scientific) and purified with either a

Table 1
Yeast strains used in this study.

Name	Relevant genotype	Parental strain	Reference
O. parapolymorpha CBS 11895 (DL-1)	Wild type		Suh and Zhou (2010)
B. bruxellensis CBS 2499	Wild-type		Smith et al. (1990)
S. cerevisiae CEN.PK113-7D	MATa *SUC2 MAL2-8*^{c}		Entian and Kötter (2007)
S. cerevisiae CEN.PK113-5D	MATa *ura3-52 SUC2 MAL2-8*^{c}		Entian and Kötter (2007)
IMX585	MATa *can1*::*Spycas9*-natNT2 *SUC2 MAL2-8*^{c}	CEN. PK113-7D	Mans et al. (2015)
IMD019	HPODL_02673^{C155CA}	CBS 11895	This study
IMD020	HPODL_02674^{G172GA}	CBS 11895	This study
IMD021	HPODL_00948^{G235GA}	CBS 11895	This study
IMD022	HPODL_00195^{C126CAT}	CBS 11895	This study
IMD023	HPODL_03424^{C229CT}	CBS 11895	This study
IMD025	*OpYNR1*^{G397GC}	CBS 11895	This study
IMD027	HPODL_01640^{C112CA}	CBS 11895	This study
IMX1777	MATa *can1*::*Spycas9*-natNT2 *sga1*:: *ScTDH3*p-HPODL_02673-*ScENO1*t *ScCCW12*p-HPODL_02674-*ScSSA1*t *ScPGK1*p-HPODL_00195-*ScADH1*t *ScHHF2*p-HPODL_01640-*ScPGK1*t *ScTEF2*p-HPODL_03424-*ScTDH1*t *ScPGM1*p-HPODL_00948-*ScPYK1*t *ScHHF1*p-HPODL_02128-*ScFBA1*t	IMX585	This study
IMX1778	MATa *can1*::*Spycas9*-natNT2 *sga1*:: *ScTDH3*p-HPODL_02673-*ScENO1*t *ScCCW12*p-HPODL_02674-*ScSSA1*t *ScPGK1*p-HPODL_00195-*ScADH1*t *ScHHF2*p-HPODL_01640-*ScPGK1*t *ScTEF2*p-HPODL_03424-*ScTDH1*t *ScPGM1*p-HPODL_00948-*ScPYK1*t *ScHHF1*p-HPODL_02128-*ScFBA1*t *ScFBA1*p-*CrMOT1*-*ScTEF2*t	IMX585	This study
IMX1779	MATa *can1*::*Spycas9*-natNT2 *sga1*:: *ScFBA1*p-*CrMOT1*-*ScTEF2*t	IMX585	This study
IMX1780	*MATa can1*::*Spycas9*-natNT2 *sga1*::*ScTEF1*p-*OpYNT1*-*ScPDC1*t *ScRPL18b*p-*OpYNR1*-*ScGPM1*t *ScTPI1*p-*OpYNI1*-*ScTPI1*t	IMX585	This study
IMX1781	MATa *can1*::*Spycas9*-natNT2 *sga1*:: *ScTDH3*p-HPODL_02673-*ScENO1*t *ScCCW12*p-HPODL_02674-*ScSSA1*t *ScPGK1*p-HPODL_00195-*ScADH1*t *ScHHF2*p-HPODL_01640-*ScPGK1*t *ScTEF2*p-HPODL_03424-*ScTDH1*t *ScPGM1*p-HPODL_00948-*ScPYK1*t *ScHHF1*p-HPODL_02128-*ScFBA1*t *ScFBA1*p-*CrMOT1*-*ScTEF2*t *ScTEF1*p-*OpYNT1*-*ScPDC1*t *ScRPL18b*p-*OpYNR1*-*ScGPM1*t *ScTPI1*p-*OpYNI1*-*ScTPI1*t	IMX585	This study
IMX1782	MATa *can1*::*Spycas9*-natNT2 *sga1*:: *ScTDH3*p-HPODL_02673-*ScENO1*t *ScCCW12*p-HPODL_02674-*ScSSA1*t *ScPGK1*p-HPODL_00195-*ScADH1*t *ScHHF2*p-HPODL_01640-*ScPGK1*t *ScTEF2*p-HPODL_03424-*ScTDH1*t *ScPGM1*p-HPODL_00948-*ScPYK1*t *ScHHF1*p-HPODL_02128-*ScFBA1*t *ScTEF1*p-*OpYNT1*-*ScPDC1*t *ScRPL18b*p-*OpYNR1*-*ScGPM1*t *ScTPI1*p-*OpYNI1*-*ScTPI1*t	IMX585	This study
IMS816	MATa *can1*::*Spycas9*-natNT2 *sga1*:: *ScTDH3*p-HPODL_02673-*ScENO1*t *ScCCW12*p-HPODL_02674-*ScSSA1*t *ScPGK1*p-HPODL_00195-*ScADH1*t *ScHHF2*p-HPODL_01640-*ScPGK1*t *ScTEF2*p-HPODL_03424-*ScTDH1*t *ScPGM1*p-HPODL_00948-*ScPYK1*t *ScHHF1*p-HPODL_02128-*ScFBA1*t *ScFBA1*p-*CrMOT1*-*ScTEF2*t *ScTEF1*p-*OpYNT1*-*ScPDC1*t *ScRPL18b*p-*OpYNR1*-*ScGPM1*t *ScTPI1*p-*OpYNI1*-*ScTPI1*t (Adapted for growth on nitrate - colony 1)	IMX1781	This study
IMS817	MATa *can1*::*Spycas9*-natNT2 *sga1*:: *ScTDH3*p-HPODL_02673-*ScENO1*t *ScCCW12*p-HPODL_02674-*ScSSA1*t *ScPGK1*p-HPODL_00195-*ScADH1*t *ScHHF2*p-HPODL_01640-*ScPGK1*t *ScTEF2*p-HPODL_03424-*ScTDH1*t *ScPGM1*p-HPODL_00948-*ScPYK1*t *ScHHF1*p-HPODL_02128-*ScFBA1*t *ScTEF1*p-*OpYNT1*-*ScPDC1*t *ScRPL18b*p-*OpYNR1*-*ScGPM1*t *ScTPI1*p-*OpYNI1*-*ScTPI1*t (Adapted for growth on nitrate - colony 1)	IMX1782	This study
IMS815	MATa *can1*::*Spycas9*-natNT2 *sga1*:: *ScTDH3*p-HPODL_02673-*ScENO1*t *ScCCW12*p-HPODL_02674-*ScSSA1*t *ScPGK1*p-HPODL_00195-*ScADH1*t *ScHHF2*p-HPODL_01640-*ScPGK1*t *ScTEF2*p-HPODL_03424-*ScTDH1*t *ScPGM1*p-HPODL_00948-*ScPYK1*t *ScHHF1*p-HPODL_02128-*ScFBA1*t *ScFBA1*p-*CrMOT1*-*ScTEF2*t *ScTEF1*p-*OpYNT1*-*ScPDC1*t *ScRPL18b*p-*OpYNR1*-*ScGPM1*t *ScTPI1*p-*OpYNI1*-*ScTPI1*t (Adapted for growth on nitrate - colony 2)	IMX1781	This study
IMS818	MATa *can1*::*Spycas9*-natNT2 *sga1*:: *ScTDH3*p-HPODL_02673-*ScENO1*t *ScCCW12*p-HPODL_02674-*ScSSA1*t *ScPGK1*p-HPODL_00195-*ScADH1*t *ScHHF2*p-HPODL_01640-*ScPGK1*t	IMX1782	This study

(*continued on next page*)

Table 1 (*continued*)

Name	Relevant genotype	Parental strain	Reference
	*ScTEF2*p-HPODL_03424-*ScTDH1*t *ScPGM1*p-HPODL_00948-*ScPYK1*t *ScHHF1*p-HPODL_02128-*ScFBA1*t *ScTEF1*p-*OpYNT1*-*ScPDC1*t *ScRPL18b*p-*OpYNR1*-*ScGPM1*t *ScTPI1*p-*OpYNI1*-*ScTPI1*t (Adapted for growth on nitrate - colony 2)		
IMS819	MATa *can1*::*Spycas9*-natNT2 *sga1*:: *ScTDH3*p-HPODL_02673-*ScENO1*t *ScCCW12*p-HPODL_02674-*ScSSA1*t *ScPGK1*p-HPODL_00195-*ScADH1*t *ScHHF2*p-HPODL_01640-*ScPGK1*t *ScTEF2*p-HPODL_03424-*ScTDH1*t *ScPGM1*p-HPODL_00948-*ScPYK1*t *ScHHF1*p-HPODL_02128-*ScFBA1*t *ScFBA1*p-*CrMOT1*-*ScTEF2*t *ScTEF1*p-*OpYNT1*-*ScPDC1*t *ScRPL18b*p-*OpYNR1*-*ScGPM1*t *ScTPI1*p-*OpYNI1*-*ScTPI1*t (Adapted for growth on nitrate - colony 3)	IMX1781	This study
IMS821	MATa *can1*::*Spycas9*-natNT2 *sga1*:: *ScTDH3*p-HPODL_02673-*ScENO1*t *ScCCW12*p-HPODL_02674-*ScSSA1*t *ScPGK1*p-HPODL_00195-*ScADH1*t *ScHHF2*p-HPODL_01640-*ScPGK1*t *ScTEF2*p-HPODL_03424-*ScTDH1*t *ScPGM1*p-HPODL_00948-*ScPYK1*t *ScHHF1*p-HPODL_02128-*ScFBA1*t *ScTEF1*p-*OpYNT1*-*ScPDC1*t *ScRPL18b*p-*OpYNR1*-*ScGPM1*t *ScTPI1*p-*OpYNI1*-*ScTPI1*t (Adapted for growth on nitrate - colony 3)	IMX1782	This study

GenElutePCR Clean-Up Kit (Sigma-Aldrich) or a Zymoclean Gel DNA Recovery Kit (Zymo Research, Irvine, CA). Plasmids were isolated from *E. coli* and *S. cerevisiae* using a Sigma GenElute HP plasmid miniprep kit (Sigma-Aldrich) or a Zymoprep Yeast Plasmid Miniprep II (Zymo Research), respectively, and verified by either restriction digestion or diagnostic PCR. *E. coli* XL1-blue was used for transformation (Inoue et al., 1990). Yeast genomic DNA used for diagnostic PCR reactions was isolated by using the SDS/LiAc protocol (Looke et al., 2011). *S. cerevisiae* transformation was performed with the LiAc method (Gietz and Woods, 2002) while *O. parapolymorpha* transformation was performed by electroporation (Juergens et al., 2018; Saraya et al., 2014). Four to eight colonies were re-streaked on selective medium to select for single clones and diagnostic PCRs were performed to verify the correct genotypes.

2.3. Identification of Moco biosynthetic genes

tBLASTn (BLOSUM62 scoring matrix, gap costs of 11 for existence and 1 for extension) analysis was performed to identify putative Moco biosynthetic genes in *O. parapolymorpha* DL-1 (Altschul et al., 1990). The protein sequences of the *E. coli* molybdopterin-cofactor biosynthesis enzymes MoaA (P30745; GTP 3′,8-cyclase), MoaC (P0A738; cyclic pyranopterin monophosphate synthase), MoeB (P12282; molybdopterin-synthase adenylyltransferase), IscS (P0A6B7; cysteine desulfurase), MoaD (P30748; molybdopterin synthase sulfur carrier subunit), MoaE (P30749; molybdopterin synthase catalytic subunit), MogA (P0AF03; molybdopterin adenylyltransferase) and MoeA (P12281; molybdopterin molybdenumtransferase) were used as query against the *O. parapolymorpha* transcriptome dataset with accession number SRX365635 (https://www.ncbi.nlm.nih.gov//sra?term=SRX365635) (Ravin et al., 2013). Identified coding sequences were manually annotated in the *O. parapolymorpha* genome sequence (PRJNA60503) and checked for the presence of alternative in-frame start codons upstream of the annotated region. Protein identity was calculated using the Clustal Omega protein alignment tool (Madeira et al., 2019).

2.4. Plasmid construction

Plasmids used in this study are shown in Table 3. Plasmids carrying two copies of the same gRNA targeting one of the putative Moco biosynthetic genes in *O. parapolymorpha* were cloned by BsaI Golden Gate assembly as previously described (Gorter de Vries et al., 2017; Juergens et al., 2018). In brief, synthetic dsDNA strings including a BsaI and ribozyme-flanked 20 bp target sequence were *de novo* synthesized and cloned in plasmids by GeneArt (Thermo Scientific). Then, each of the plasmids pUD697, pUD698, pUD699, pUD700, pUD701, pUD703, pUD704, and pUD705 carrying the gRNA sequence targeting HPODL_02673, HPODL_02674, HPODL_00948, HPODL_00195, HPODL_03424, *OpYNR1*, HPODL_02128, and HPODL_01640, respectively, was combined in a 'one pot' BsaI Golden Gate reaction (Engler et al., 2008) together with the backbone carrying plasmid pUDP002 (Addgene plasmid number #103872) (Juergens et al., 2018) to yield plasmids pUDP093 ($gRNA_{HPODL\_02673}$) pUDP094 ($gRNA_{HPODL\_02674}$), pUDP095 ($gRNA_{HPODL\_00948}$), pUDP096 ($gRNA_{HPODL\_00195}$), pUDP097 ($gRNA_{HPODL\_03424}$), pUDP099 ($gRNA_{OpYNR1}$), pUDP100 ($gRNA_{HPODL\_02128}$), and pUDP101 ($gRNA_{HPODL\_01640}$), respectively.

In order to assemble plasmids with promoter-gene-terminator expression modules, new promoters and terminator parts compatible with the Golden Gate based yeast toolkit (YTK) were cloned (Lee et al., 2015). For this purpose, terminator parts from *S. cerevisiae* were amplified with primers having YTK-compatible ends and *S. cerevisiae* CEN. PK113-7D genomic DNA as template. Primer pairs 10886/10887, 10765/10766, 10757/10758, 10773/10774, and 10759/10760 were used to amplify *ScPYK1t*, *ScTPI1t*, *ScFBA1t*, *ScPDC1t*, and *ScGPM1t*, respectively and purified PCR products were used in a BsmBI Golden Gate reaction together with the pUD565 entry vector to yield pGGKp040, pGGKp042, pGGKp046, and pGGKp048, respectively. Plasmids carrying *ScFBA1p*, *ScTPI1p*, *ScGPM1p* flanked by YTK compatible ends, were *de novo* synthesized by GeneArt (Thermo Scientific) and named pGGKp104, pGGKp114, and pGGKp116, respectively. Promoter fragments of glycolytic genes were selected to be 800 bp long while terminator length was selected to be 300 bp.

Plasmids carrying a transcriptional unit for expression in *S. cerevisiae* were cloned by either Golden Gate assembly, Gibson assembly or *in vivo* homologous recombination in yeast. All coding sequences were amplified from *O. parapolymorpha* DL-1 genomic DNA (gDNA) as template, except for the *Chlamydomonas reinhardtii MOT1* gene, which was codon optimized for expression in *S. cerevisiae* and *de novo* synthesized by GeneArt (Thermo Scientific) resulting in plasmid pUD728. Expression cassettes for HPODL_02674, HPODL_00195, HPODL_01640, HPODL_03424, *CrMOT1*, *OpYNT1*, and *OpYNR1* were constructed *in vitro* by Golden Gate assembly (Lee et al., 2015). First, primer pairs 12871/12872, 12873/12874, 12875/12876, 12879/12880, 12881/12882, 12899/12900, and 12901/12902 were used to amplify the HPODL_02674, HPODL_00195, HPODL_01640, HPODL_03424, *CrMOT1*, *OpYNT1*, and *OpYNR1* coding sequence, respectively, to add the YTK part 3 compatible ends. Then, each linear DNA carrying the coding sequence for HPODL_02674, HPODL_00195, HPODL_01640, HPODL_03424, *CrMOT1*, *OpYNT1*, and *OpYNR1* was combined together with the backbone plasmid pYTK096 and the respective promoter/terminator part plasmid pair pYTK010/pYTK052, pYTK011/pYTK055, pYTK012/pYTK054, pYTK014/pYTK056, pGGKp104/pGGKp038, pYTK013/pGGKp045, and pYTK017/pGGKp048,

Table 2
Primers used in this study.

Primer number	Primer sequence	Product(s)
12251	Tgcgccttgatacgtgc	HPODL_02673_InDelCheck_fwd
12252	Aaataagaaggagaaacatgcagg	HPODL_02674_InDelCheck_fwd And internal junction 1 check
12253	Acatcctccctcaagtagtagcc	HPODL_00948_InDelCheck_fwd
12254	Gactggtgttagacaaaccgg	HPODL_00195_InDelCheck_fwd
12255	Tgctcgaccatctcgagc	HPODL_03424_InDelCheck_fwd
12257	Caccatggtcggaagaacc	*YNR1*_InDelCheck_fwd
12259	Gcgtaaacaacatgtccacc	HPODL_01640_InDelCheck_fwd
12260	Gtatgtcctcgtatgagaccagc	HPODL_02673_InDelCheck_rev
12261	Cgattgagagagctttttggc	HPODL_02674_InDelCheck_rev
12262	cctgttcagagaaagagaagcc	HPODL_00948_InDelCheck_rev
12263	ggacgtactgcgaaatctgg	HPODL_00195_InDelCheck_rev
12264	gattacttctggagctggcg	HPODL_03424_InDelCheck_rev
12266	atgtaattcctcacgaactttgg	*YNR1*_InDelCheck_rev
12268	aagccgggtcttctttcc	HPODL_01640_InDelCheck_rev
12863	ggtcacccatgtatgctggaaatctgctcgtca	pYTK096_backbone_gibson_pUDI189_FWD
12864	gataatgataaactcgaactgcgttgtattgcgacgaattg	pYTK096_backbone_gibson_pUDI189_REV
12865	tcgtcgcaatacaacgcagttcgagtttatcattatc	pYTK009_promoter_gibson_pUDI189_FWD
12866	cagcagtaatgaggatatcatagatcttttgtttgtttatgtgtgtttattc	pYTK009_promoter_gibson_pUDI189_REV
12867	cataaacaaacaaaagatctatgatatcctcattactgctgaggc	HPODL_02673_insert_gibson_pUDI189_FWD
12868	aaagctctcgagttaGGATtcaTCCTCCAATTAAAATCATCG	HPODL_02673_insert_gibson_pUDI189_REV
12869	TGATTTTAATTGGAGGAtgaATCCtaactcgagagcttttgattaag	pYTK051_terminator_gibson_pUDI189_FWD
12870	cgagcagatttccagcatacatgggtgaccaa	pYTK051_terminator_gibson_pUDI189_FWD _REV
12871	GCATCGTCTCATCGGTCTCATatggttgcaattcatgaaaaaga	HPODL_02674_Insert_goldengate_pUDI190_FWD
12872	TGCCGTCTCAGGTCTCAGGATctatttgaagatggttgatagatctatgtc	HPODL_02674_Insert_goldengate_pUDI190_REV
12873	GCATCGTCTCATCGGTCTCATatgtccatctttgtagatattactgataagc	HPODL_00195_Insert_goldengate_pUDI191_FWD
12874	TGCCGTCTCAGGTCTCAGGATttaggtgcgactaagcacgttag	HPODL_00195_Insert_goldengate_pUDI191_REV
12875	GCATCGTCTCATCGGTCTCATatggtcgcagttgctatcga	HPODL_01640_Insert_goldengate_pUDI192_FWD
12876	TGCCGTCTCAGGTCTCAGGATttatccacttgaaactggcgg	HPODL_01640_Insert_goldengate_pUDI192_REV
12879	GCATCGTCTCATCGGTCTCATatgactgttggtatcttggttgtatca	HPODL_03424_Insert_goldengate_pUDI194_FWD
12880	TGCCGTCTCAGGTCTCAGGATtcacacatagatctggtcgatgaga	HPODL_03424_Insert_goldengate_pUDI194_REV
12881	GCATCGTCTCATCGGTCTC	*CrMOT1*_insert_goldengate_pUDI195_FWD
12882	TGCCGTCTCAGGTCTCAGGATTTAAGCTCTACCACCTCTAGCAAAAAC	*CrMOT1*_insert_goldengate_pUDI195_REV
12883	GGATGGCGAAAGGATACGCTGgaaatctgctcgtcag	pGGK d017_backbone_*in vivo* assembly_pUDE796_FWD
12884	CCTGTCAAAGTATCACcgttgtattgcgacgaattgc	pGGKd017_backbone_*in vivo* assembly_pUDE796_REV
12885	tcgtcgcaatacaacgGTGATACTTTGACAGGAGC	pGGKp116_promoter_*in vivo* assembly_pUDE796_FWD
12886	ctcatttaaggacaaagaCATATATTGTAATATGTGTGTTTGTTTGGATT	pGGKp116_promoter_*in vivo* assembly_pUDE796_REV
12887	ACAAACACACATATTACAATATATGtctttgtccttaaatgagtaccttcg	HPODL_00948_insert_*in vivo* assembly_pUDE796_FWD
12888	AATCATGATTCTTTTTGGATttagtaaatagggaagtttgggtctatctg	HPODL_00948_insert_*in vivo* assembly_pUDE796_REV
12889	ccaaacttccctatttactaaATCCAAAAAGAATCATGATTGAATG	pGGKp038_terminator_*in vivo* assembly_pUDE796_FWD
12890	acgagcagatttcCAGCGTATCCTTTCGCCA	pGGKp038_terminator_*in vivo* assembly_pUDE796_REV
12891	GAGTTCGCGGCTGgaaatctgctcgtcag	pYTK096_backbone_gibson_pUDI197_FWD
12892	gtaaggccccaagacgttgtattgcgacgaattg	pYTK096_backbone_gibson_pUDI197_REV
12893	gcaattcgtcgcaatacaacgtcttggggccttaccacc	pYTK015_promoter_gibson_pUDI197_FWD
12894	cgatcctgaacctgtacatagatctattttactatattatatttgttgcttgt	pYTK015_promoter_gibson_pUDI197_REV
12895	caacaaatataatatagtaaaatagatctatgtacaggttcaggatcgga	HPODL_02128_Insert_gibson_FWD
12896	CAATTAATTTGAATTAACGGATtcaatgtcctgcccattcg	HPODL_02128_Insert_gibson_REV
12897	tgggcaggacattgaATCCGTTAATTCAAATTAATTGATATAGTTTT	pGGKp040_terminator_gibson_pUDI197_FWD
12898	acgagcagatttcCAGCCGCGAACTCCAA	pGGKp040_terminator_gibson_pUDI197_REV
12899	GCATCGTCTCATCGGTCTCATATGCGACTTTCTACCTTATGGGA	*YNT1*_insert_goldengate_FWD_pUDI198
12900	TGCCGTCTCAGGTCTCAGGATTCAAATTTCCGCTTTCCTAGG	*YNT1*_insert _goldengate_REV_pUDI198
12901	GCATCGTCTCATCGGTCTCATatggactctgttgtcactgaggtg	*YNR1*_insert _goldengate_FWD_pUDI199
12902	TGCCGTCTCAGGTCTCAGGATtcagaagtacactacatactgtttatccaaa	*YNR1*_insert _goldengate_REV_pUDI199
12903	AGAAGTGTACCGGCTGgaaatctgctcgtcag	pGGKd017_backbone_*in vivo* assembly_pUDE797_FWD
12904	ATCTCTGGGTCTTcgttgtattgcgacgaattg	pGGKd017_backbone_*in vivo* assembly_pUDE797_REV

(*continued on next page*)

Table 2 (*continued*)

Primer number	Primer sequence	Product(s)
12905	cgtcgcaatacaacgAAGACCCAGAGATGTTGT	pGGKp114_promoter_*in vivo* assembly_pUDE797_FWD
12906	GAGGAACAGAACAAGTCATATTTTAGTTTATGTATGTGTTTTTTGTAGTTATAG	pGGKp114_promoter_*in vivo* assembly_pUDE797_REV
12907	CAAAAAACACATACATAAACTAAAATATGACTTGTTCTGTTCCTCCCTT	*YNI1*_insert_*in vivo* assembly_pUDE797_FWD
12908	TTTTTATATAATTATATTAATCGGATTTACCAGTCGAACGATATTGCTTTG	*YNI1*_insert_*in vivo* assembly_pUDE797_REV
12909	CGTTCGACTGGTAAATCCGATTAATATAATTATATAAAAATATTATCTTCTTTTC	pGGKp042_terminator_*in vivo*_assembly_pUDE797_FWD
12910	cactgacgagcagatttcCAGCCGGTACACTTCTGAGTAAC	pGGKp042_terminator_*in vivo* assembly_pUDE797_REV
13123	TTTACAATATAGTGATAATCGTGGACTAGAGCAAGATTTCAAATAAGTAACAGCAGCAAAcagttcgagtttatcattatcaatactg	SGA1_homology_pUDI189_cassette_integration_fwd
13124	ATAGCATAGGTGCAAGGCTCTCGCCGCTTGTCGAGCTATTGGCATGGATGTGCTCCCTAAatacatgggtgaccaaaagagc	SHR1__homology_pUDI189_cassette_integration_rev
13125	TTAGGGAGCACATCCATGCCAATAGCTCGACAAGCGGCGAGAGCCTTGCACCTATGCTATcacccatgaaccacacgg	SHR1__homology_pUDI190_cassette_integration_fwd
13126	TCAGCGTGTTGTAATGATGCGCCATGAATTAGAATGCGTGATGATGTGCAAAGTGCCGTCataaaattaaagtagcagtacttcaaccattag	SHR2_homology_pUDI190_cassette_integration_rev
13127	GACGGCACTTTGCACATCATCACGCATTCTAATTCATGGCGCATCATTACAACACGCTGAgtgagtaaggaaagagtgaggaact	SHR2__homology_pUDI191_cassette_integration_fwd
13128	GCTACATCTTCCGTACTATGCTGTAGTCTCATGGTCGAGTTCTATTGCTGTTCGGCGGCAgaaaatggggagcgatttg	SHR3_homology_pUDI191_cassette_integration_rev
13129	TGCCGCCGAACAGCAATAGAACTCGACCATGAGACTACAGCATAGTACGGAAGATGTAGCtgtggagtgtttgcttggattct	SHR3_homology_pUDI192_cassette_integration_fwd
13130	CTCCACTGTACTGCATGTAGCATTCGCCGATCTGCATGATGTGTGACATTCTGCTATCGGacatagaaatatcgaatgggaaaaaaaaac	SHR4_homology_pUDI192_cassette_integration_rev
13131	CCGATAGCAGAATGTCACACATCATGCAGATCGGCGAATGCTACATGCAGTACAGTGGAGttgataggtcaagatcaatgtaaacaat	SHR4_homology_pUDI194_cassette_integration _fwd
13132	TGAGAGCTTGTGATAACTGCTCGCCAGTTGTGGTGATCTCCCAGTCGGTGTAGCAGCAATcgttcagggtaatatattttaaccg	SHR6_homology_pUDI194_cassette_integration _rev
13133	ATTGCTGCTACACCGACTGGGAGATCACCACAACTGGCGAGCAGTTATCACAAGCTCTCAGTGATACTTTGACAGGAGCTATATCATG	SHR6_homology_pUDE796_cassette_integration_fwd
13134	GGTGAATTGAGAGCTATCCTATATTATAGCAGATGCCGGGTATGCAGCTTGGTAGAATGCGTATCCTTTCGCCATCCTGATA	SHR7_homology_pUDE796_cassette_integration _rev
13135	GCATTCTACCAAGCTGCATACCCGGCATCTGCTATAATATAGGATAGCTCTCAATTCACCtcttggggccttaccacc	SHR7_homology_pUDI197_cassette_integration_fwd
13136	CTCAGCCTTAGCCAATATGATCATGTCGTTGCGTCTCGGACCATCTAGTCTACTCTGAAGCGCGAACTCCAAAATGAGC	SHR8_homology_pUDI197_cassette_integration_rev
13570	TATATTTGATGTAAATATCTAGGAAATACACTTGTGTATACTTCTCGCTTTTCTTTTATTCGCGAACTCCAAAATGAGC	SGA1_homology_pUDI197_cassette_integration_rev
13573	CAGTGACGTGAGTGCCATCTGCAGGTCATGTGATGCTATCAGCTACACTGCCAGCAATGACGCGAACTCCAAAATGAGC	SHR9_homology_pUDI197_cassette_integration_ rev
13138	TTTACAATATAGTGATAATCGTGGACTAGAGCAAGATTTCAAATAAGTAACAGCAGCAAATGAACAACAATACCAGCCTTCC	SGA1_homology_pUDI196_cassette_integration_fwd
13139	CTTCAGAGTAGACTAGATGGTCCGAGACGCAACGACATGATCATATTGGCTAAGGCTGAGTGAACAACAATACCAGCCTTCC	SHR8_homology_pUDI196_cassette_integration_fwd
13571	TATATTTGATGTAAATATCTAGGAAATACACTTGTGTATACTTCTCGCTTTTCTTTTATTAGGAAACGTAAATTACAAGGTATATACATACG	SGA1_homology_pUDI196_cassette_integration_rev
13141	CAGTGACGTGAGTGCCATCTGCAGGTCATGTGATGCTATCAGCTACACTGCCAGCAATGAAGGAAACGTAAATTACAAGGTATATACATACG	SHR9_homology_pUDI196_cassette_integration_rev
13142	TTTACAATATAGTGATAATCGTGGACTAGAGCAAGATTTCAAATAAGTAACAGCAGCAAAccttgccaacagggagttc	SGA1_homology_pUDI198_cassette_integration_fwd
13143	TCATTGCTGGCAGTGTAGCTGATAGCATCACATGACCTGCAGATGGCACTCACGTCACTGccttgccaacagggagttc	SHR9_homology_pUDI198_cassette_integration_fwd
13144	ACGCAATATCGGCCATCGTGCGAGTGTCTCAAACTATCTGTATGCAAATTCGTGCGTGTGCAGTGTTCCTTAATCAAGGATACCTC	SHR10_homology_pUDI198_cassette_integration rev
13145	CACACGCACGAATTTGCATACAGATAGTTTGAGACACTCGCACGATGGCCGATATTGCGTaagaggatgtccaatatttttttaag	SHR10_homology_pUDI199_cassette_integration_fwd
13146	TCAGACAATTCTATACGCGGACTGATATGGCAGAAGCTAGGAGACGTTATGCGATCTTAGCATTAAACTACGATGTAAACATCAAGG	SHR11_homology_pUDI199_cassette_integration _rev
13147	CTAAGATCGCATAACGTCTCCTAGCTTCTGCCATATCAGTCCGCGTATAGAATTGTCTGAAAGACCCAGAGATGTTGTTGTC	SHR11_homology_pUDE797_cassette_integration_fwd
13572	TATATTTGATGTAAATATCTAGGAAATACACTTGTGTATACTTCTCGCTTTTCTTTTATTCGGTACACTTCTGAGTAACCCATATAG	SGA1_homology_pUDE797_cassette_integration_rev
3372	GCCCAAATCGGCATCTTTAAATG	Internal_junction_1_check_REV
13727	ccaattggtgcggcaattg	Internal_junction_2_check_FWD
13728	aaacaaatcacgagcgacgg	Internal_junction_2_check_REV
13729	gttgctttctcaggtatagcatgagg	Internal_junction_3_check_FWD
13730	gcgaaactctcggtctagtacc	Internal_junction_3_check_REV
13731	cttttctctttccccatcctttacg	Internal_junction_4_check_FWD
13732	cgccgtcacaaacaacc	Internal_junction_4_check_REV
13733	gttatggcgagaacgtcgg	Internal_junction_5_check_FWD
13734	GCATCACTGCATGTGTTAACCG	Internal_junction_5_check_REV
13735	TCCAATTGTCGTCATAACGATGAGG	Internal_junction_6_check_FWD
13736	gatcctggccgtaatatctctcc	Internal_junction_6_check_REV
13737	GTCGGCTCTTTTCTTCTGAAGG	Internal_junction_7_check_FWD
13738	TTAGGGCTTGCGTCAGC	Internal_junction_7_check_REV
13739	ATGTCCTCCAACTCGGC	Internal_junction_8_check_FWD
13740	cggagtccgagaaaatctgg	Internal_junction_8_check_REV
13741	GAATTGGCTTAAGTCTGGGTCC	Internal_junction_9_check_FWD
13742	cgttctcaagacgtggtcc	Internal_junction_9_check_REV
13743	TTTTCAGCCTGTCGTGGTAGC	Internal_junction_10_check_FWD
13744	AGGGAATAAGTAGGGTGATACCGC	Internal_junction_10_check_REV
7806	ACTCGAAGCAGTTCAGAACG	5′ External_junction_1_2_3_check_FWD
4369	GAGGCACATCTGCGTTTCAGG	5′ External_junction_1_check_REV
5026	CGTATTACGATAATCCTGCTGTC	5′ External_junction_2_check_REV

(*continued on next page*)

Table 2 (*continued*)

Primer number	Primer sequence	Product(s)
8410	CGACGAAGAAAAAGAAACGAGG	5′ External_junction_3_check_REV
2372	TATTGGTCGGCTCTTTTCTTCTG	3′ External_junction_1_check_FWD
5389	GTTCTTCCTTGCGTTATTCTTCTG	3′ External_junction_2_check_FWD
2375	TGAGCCACTTAAATTTCGTGAATG	3′ External_junction_3_check_FWD
7331	GAGACTCGCATGAGAACATC	3′ External_junction_1_2_3_check_REV
10886	AAGCATCGTCTCATCGGTCTCAATCCAAAAAGAATCATGATTGAATGAAGATATT	*ScPYK1t*_YTK_fwd
10887	TTATGCCGTCTCAGGTCTCACAGCGTATCCTTTCGCCATCCTG	*ScPYK1t*_YTK_rev
10765	AAGCATCGTCTCATCGGTCTCAATCCGATTAATATAAATTATTATCTTCTTTTC	*ScTPI1t*_YTK_fwd
10766	TTATGCCGTCTCAGGTCTCACAGCCGGTACACTTCTGAGTAAC	*ScTPI1t*_YTK_rev
10757	AAGCATCGTCTCATCGGTCTCAATCCGTTAATTCAAATTAATTGATATAGTTTTTTAATG	*ScFBA1t*_YTK_fwd
10758	TTATGCCGTCTCAGGTCTCACAGCCGCGAACTCCAAAATGAGC	*ScFBA1t*_YTK_rev
10773	AAGCATCGTCTCATCGGTCTCAATCCGCGATTTAATCTCTAATTATTAGTTAAAG	*ScPDC1t*_YTK_fwd
10774	TTATGCCGTCTCAGGTCTCACAGCCAGTGTTCCTTAATCAAGGATACC	*ScPDC1t*_YTK_rev
10759	AAGCATCGTCTCATCGGTCTCAATCCGTCTGAAGAATGAATGATTTGATG	*ScGPM1t*_YTK_fwd
10760	TTATGCCGTCTCAGGTCTCAGCCATTAAACTACGATGTAAACATC	*ScGPM1t*_YTK_rev

Table 3
Plasmids used in this study.

Name	Characteristics	Reference
pUDP002	ori bla panARS(OPT) *AgTEF1*p-hph-*AgTEF1t* *ScTDH3p*$^{BsaI\ BsaI}$*ScCYC1t AaTEF1p-Spycas9*$^{D147Y\ P411T}$*-ScPHO5t*	Juergens et al. (2018)
pYTK096	3′*URA3* ConLS′ *gfp* ConRE′*URA3 ntpII* ColE1 5′*URA3*	Lee et al. (2015)
pGGKd017	ConLS′ *gfp* ConRE′ *URA3* 2 μm *bla* ColE1	Wronska et al. (2020)
pYTK009	*cat* ColE1 ^{BsaI}-*ScTDH3*p-^{BsaI}	Lee et al. (2015)
pYTK010	*cat* ColE1 ^{BsaI}-*ScCCW12*p-^{BsaI}	Lee et al. (2015)
pYTK011	*cat* ColE1 ^{BsaI}-*ScPGK1*p-^{BsaI}	Lee et al. (2015)
pYTK012	*cat* ColE1 ^{BsaI}-*ScHHF2*p-^{BsaI}	Lee et al. (2015)
pYTK013	*cat* ColE1 ^{BsaI}-*ScTEF1*p-^{BsaI}	Lee et al. (2015)
pYTK014	*cat* ColE1 ^{BsaI}-*ScTEF2*p-^{BsaI}	Lee et al. (2015)
pYTK015	*cat* ColE1 ^{BsaI}-*ScHHF1*p-^{BsaI}	Lee et al. (2015)
pYTK017	*cat* ColE1 ^{BsaI}-*ScRPL18b*p-^{BsaI}	Lee et al. (2015)
pYTK051	*cat* ColE1 ^{BsaI}-*ScENO1*t-^{BsaI}	Lee et al. (2015)
pYTK052	*cat* ColE1 ^{BsaI}-*ScSSA1*t-^{BsaI}	Lee et al. (2015)
pYTK053	*cat* ColE1 ^{BsaI}-*ScADH1*t-^{BsaI}	Lee et al. (2015)
pYTK054	*cat* ColE1 ^{BsaI}-*ScPGK1*t-^{BsaI}	Lee et al. (2015)
pYTK055	*cat* ColE1 ^{BsaI}-*ScENO2*t-^{BsaI}	Lee et al. (2015)
pYTK056	*cat* ColE1 ^{BsaI}-*ScTDH1*t-^{BsaI}	Lee et al. (2015)
pUDR119	2 μm amdSYM *SNR52*p-gRNA.*SGA1*.Y-*SUP4*t	van Rossum et al. (2016)
pROS 13	2 μm *bla* kanMX gRNA-*CAN1*.Y gRNA-*ADE2*.Y	Mans et al. (2015)
pUD565	*cat* ColE1	Boonekamp et al. (2018)
pUD697	*bla* ColE1 ^{BsaI}HH-gRNA$_{HPODL_02673}$-HDV^{BsaI}	GeneArt, this study
pUD698	*bla* ColE1 ^{BsaI}HH-gRNA $_{HPODL\_02674}$-HDV^{BsaI}	GeneArt, this study
pUD699	*bla* ColE1 ^{BsaI}HH-gRNA$_{HPODL_00948}$-HDV^{BsaI}	GeneArt, this study
pUD700	*bla* ColE1 ^{BsaI}HH-gRNA $_{HPODL\_00195}$-HDV^{BsaI}	GeneArt, this study
pUD701	*bla* ColE1 ^{BsaI}HH-gRNA $_{HPODL\_03424}$-HDV^{BsaI}	GeneArt, this study
pUD703	*bla* ColE1 ^{BsaI}HH-gRNA $_{YNR1}$-HDV^{BsaI}	GeneArt, this study
pUD704	*bla* ColE1 ^{BsaI}HH-gRNA $_{HPODL\_02128}$-HDV^{BsaI}	GeneArt, this study
pUD705	*bla* ColE1 ^{BsaI}HH-gRNA $_{HPODL\_01640}$-HDV^{BsaI}	GeneArt, this study
pUD728	*bla* ColE1 ^{BsaI}-*CrMOT1*-^{BsaI}	GeneArt, this study
pUDP093	*bla* ColE1 panARS(OPT) *AgTEF1*p-hph-*AgTEF1*t *ScTDH3*p–HH– gRNA$_{HPODL_02673}$-HDV-*ScCYC1*t *AaTEF1*p-*Spycas9*$^{D147Y\ P411T}$*-ScPHO5*t	This study
pUDP094	*bla* ColE1 panARS(OPT) *AgTEF1*p-hph-*AgTEF1*t *ScTDH3*p–HH– gRNA$_{HPODL_02674}$-HDV-*ScCYC1*t *AaTEF1*p-*Spycas9*$^{D147Y\ P411T}$*-ScPHO5*t	This study
pUDP095	*bla* ColE1 panARS(OPT) *AgTEF1*p-hph-*AgTEF1*t *ScTDH3*p–HH– gRNA$_{HPODL_00948}$-HDV-*ScCYC1*t *AaTEF1*p-*Spycas9*$^{D147Y\ P411T}$*-ScPHO5*t	This study
pUDP096	*bla* ColE1 panARS(OPT) *AgTEF1*p-hph-*AgTEF1*t *ScTDH3*p–HH– gRNA $_{HPODL\_00195}$-HDV-*ScCYC1*t *AaTEF1*p-*Spycas9*$^{D147Y\ P411T}$*-ScPHO5*t	This study
pUDP097	*bla* ColE1 panARS(OPT) *AgTEF1*p-hph-*AgTEF1*t *ScTDH3*p–HH– gRNA$_{HPODL_03424}$-HDV-*ScCYC1*t *AaTEF1*p-*Spycas9*$^{D147Y\ P411T}$*-ScPHO5*t	This study
pUDP099	*bla* ColE1 panARS(OPT) *AgTEF1*p-hph-*AgTEF1*t *ScTDH3*p–HH– gRNA$_{OpYNR1}$-HDV-*ScCYC1*t *AaTEF1*p-*Spycas9*$^{D147Y\ P411T}$*-ScPHO5*t	This study
pUDP100	*bla* ColE1 panARS(OPT) *AgTEF1*p-hph-*AgTEF1*t *ScTDH3*p–HH–gRNA $_{HPODL\_02128}$-HDV-*ScCYC1*t *AaTEF1*p-*Spycas9*$^{D147Y\ P411T}$*-ScPHO5*t	This study
pUDP101	*bla* ColE1 panARS(OPT) *AgTEF1*p-hph-*AgTEF1*t *ScTDH3*p–HH–gRNA $_{HPODL\_01640}$-HDV-*ScCYC1*t *AaTEF1*p-*Spcas9*$^{D147Y\ P411T}$*-ScPHO5*t	This study
pGGKp040	*cat* ColE1 ^{BsaI}-*ScPYK1*t-^{BsaI}	This study
pGGKp042	*cat* ColE1 ^{BsaI}-*ScTPI1*t-^{BsaI}	This study
pGGKp045	*cat* ColE1 ^{BsaI}-*ScPDC1*t-^{BsaI}	This study
pGGKp046	*cat* ColE1 ^{BsaI}-*ScFBA1*t-^{BsaI}	This study
pGGKp048	*cat* ColE1 ^{BsaI}-*ScGPM1*t-^{BsaI}	This study

(*continued on next page*)

Table 3 (*continued*)

Name	Characteristics	Reference
pGGKp104	*cat* ColE1 ^{BsaI}-*ScFBA1*p-^{BsaI}	This study
pGGKp114	*cat* ColE1 ^{BsaI}-*ScTPI1*p-^{BsaI}	This study
pGGKp116	*cat* ColE1 ^{BsaI}-*ScGPM1*p-^{BsaI}	This study
pUDI189	3′*URA3* ConLS′ *ScTDH3*p-HPODL_02673-*ScENO1*t ConRE′*URA3 ntpII* ColE1 5′*URA3*	This study
pUDI190	3′*URA3* ConLS′ *ScCCW12*p-HPODL_02674-*ScSSA1*t ConRE′*URA3 ntpII* ColE1 5′*URA3*	This study
pUDI191	3′*URA3* ConLS′ *ScPGK1*p-HPODL_00195-*ScADH1*t ConRE′*URA3 ntpII* ColE1 5′*URA3*	This study
pUDI192	3′*URA3* ConLS′ *ScHHF2*p-HPODL_01640-*ScPGK1*t ConRE′*URA3 ntpII* ColE1 5′*URA3*	This study
pUDI193	3′*URA3* ConLS′ *ScTEF1*p-HPODL_00337-*ScENO2*t ConRE′*URA3 ntpII* ColE1 5′*URA3*	This study
pUDI194	3′*URA3* ConLS′ *ScTEF2*p-HPODL_03424-*ScTDH1*t ConRE′*URA3 ntpII* ColE1 5′*URA3*	This study
pUDI195	3′*URA3* ConLS′ *ScFBA1*p-*CrMOT1-ScTEF2*t ConRE′*URA3 ntpII* ColE1 5′*URA3*	This study
pUDE796	ConLS′ *ScGPM1*p-HPODL_00948-*ScPYK1*t ConRE′ *URA3* 2 μm *bla* ColE1	This study
pUDI197	3′*URA3* ConLS′ *ScHHF1*p-HPODL_02128-*ScFBA1*t i ConRE′*URA3 ntpII* ColE1 5′*URA3*	This study
pUDI198	3′*URA3* ConLS′ *ScTEF1*p-*OpYNT1-ScPDC1*t ConRE′*URA3 ntpII* ColE1 5′*URA3*	This study
pUDI199	3′*URA3* ConLS′ *ScRPL18*bp-*OpYNR1-ScGPM1*t ConRE′*URA3 ntpII* ColE1 5′*URA3*	This study
pUDE797	ConLS′ *ScTPI1*p-*OpYNI1-ScTPI1*t ConRE′ *URA3* 2 μm *bla* ColE1	This study
pUDR653	2 μm *bla* kanMX gRNA-*OpYNR1*.Y gRNA-*OpYNR1*.Y	This study

in a BsaI Golden gate reaction to yield pUDI190, pUDI191, pUDI192, pUDI194, pUDI195, pUDI198, and pUDI199, respectively. The expression cassettes for HPODL_02673 and HPODL_02128 were constructed using *in vitro* Gibson assembly (Gibson et al., 2009). *ScTDH3p* promoter, HPODL_02673 coding sequence, *ScSSA1t* terminator and backbone were amplified using primer pairs 12865/12866, 12867/12868, 12869/12870, 12863/12864 and pYTK009, *O. parapolymorpha* DL-1 gDNA, pYTK055 and pYTK096 as template, respectively. PCR products were then combined in equimolar amounts in an *in vitro* Gibson assembly reaction with NEBuilder HiFi DNA Assembly Master Mix (New England Biolabs, Ipswich, MA) that yielded plasmid pUDI189. Similarly, *ScHHF1p* promoter, HPODL_02128 coding sequence, *ScFBA1t* terminator and backbone fragments were amplified with primer pairs 12893/12894, 12895/12896, 12897/12898, 12891/12892 and pYTK015, *O. parapolymorpha* DL-1 gDNA, pGGKp040 and pYTK096 as template, respectively. Equimolar amounts of these PCR products were then combined in an *in vitro* Gibson assembly reaction that yielded plasmid pUDI197. The expression cassettes for HPODL_00948 and *OpYNI1* (HPODL_02386) were constructed using *in vivo* assembly in *S. cerevisiae* (Raymond et al., 1999). *ScGPM1p* promoter, HPODL_00948 coding sequence, *ScPYK1t* terminator and backbone were amplified using primer pairs 12885/12886, 12887/12888, 12889/12890, 12883/12884 and *O. parapolymorpha* DL-1 gDNA, pGGKp038, and pGGKd017 as template, respectively. *S. cerevisiae* CEN. PK113-5D (*MATa ura3-52*) was then co-transformed with equimolar amounts of PCR products to yield pUDE796. Similarly, *ScTPI1p* promoter, HPODL_02386 (*OpYNI1*) coding sequence, *ScTPI1t* terminator and backbone were amplified using primer pairs 12893/12894, 12895/12896, 12897/12898, 12891/12892 and pGGKp114, *O. parapolymorpha* DL-1 gDNA, pGGKp040, and pGGKd017 as template, respectively. *S. cerevisiae* CEN. PK113-5D (*MATa ura3-52*) was then transformed with equimolar amounts of PCR products to yield pUDE797.

2.5. Strain construction

O. parapolymorpha strains carrying a single gene disruption were obtained by transformation with the gRNA- and Cas9-carrying plasmid followed by prolonged incubation in selective media as previously described (Juergens et al., 2018). *O. parapolymorpha* DL-1 strain (CBS 11895) was individually transformed with plasmids pUDP093, pUDP094, pUDP095, pUDP096, pUDP097, pUDP099, and pUDP101 to yield strains IMD019 (HPODL_02673^{C155CA}), IMD020 (HPODL_02674^{G172GA}), IMD021 (HPODL_00948^{G235GA}), IMD022 (HPODL_00195^{C126CAT}), IMD023 (HPODL_03424^{C229CT}), IMD025 (*OpYNR1*^{G397GC}), and IMD027 (HPODL_01640^{C112CA}), respectively. Editing at HPODL_02673, HPODL_02674, HPODL_00948, HPODL_00195, HPODL_03424, *OpYNR1*, HPODL_01640 was verified by PCR amplification of each *locus* using primer pairs 12251/12260, 12252/12261, 12253/12262, 12254/12263, 12255/12264, 12257/12266, and 12258/12268, respectively. Resulting DNA fragments were purified, and Sanger sequenced (Baseclear, Leiden, The Netherlands) to check for the presence of INDELs.

S. cerevisiae strains carrying different combinations of the Moco, Mo-transport, and nitrate modules were obtained by co-transforming strain IMX585 (*MATa Cas9*) with the gRNA^{SGA1} targeting plasmid pUDR119 together equimolar amounts of each expression cassette that was previously amplified by PCR to add unique 60 bp homology flanks. Transformants were selected by plating on SMD_{Ac} solid medium (Solis-Escalante et al., 2013). Correct integration of expression cassettes was assessed by PCR amplification of each recombination junction. Primers used for integration fragments and junction-check PCR reactions are given in Supplementary Figs. S1–6. Following genotyping of transformants, gRNA-carrying plasmids were cured (Mans et al., 2015). For each transformation, one correctly genotyped clone was stocked at −80 °C and named IMX1777 (Moco), IMX1778 (Moco, Mo-transport), IMX1779 (Mo importer), IMX1780 (nitrate), IMX1781 (Moco, Mo-transport, nitrate), IMX1782 (Moco, nitrate).

2.6. O. parapolymorpha spot-plate assay

Frozen aliquots of *O. parapolymorpha* strains IMD019-23, IMD025 and IMD027, as well as of reference strains *S. cerevisiae* CEN. PK113-7D and *O. parapolymorpha* DL-1 were thawed and used to inoculate 20 mL SMD_{Amm} flask cultures. Once OD_{660} reached a value above 5, cultures were spun down at 3000 g for 5 min. Cell pellets were washed thrice with sterile demineralized water and resuspended to an OD_{660} of 1. For each strain, 10 μL aliquots of the resulting suspension was spotted on either SMD_{Amm} or SMD_{NO3} agar plates. Photographs were taken after 48 h incubation at 30 °C.

2.7. Aerobic shake flask experiments

To adapt engineered *S. cerevisiae* strains IMX1777-1782 for growth on nitrate, they were inoculated in triplicate in 20 mL SMD_{NO3} in 100 mL flasks until, after approximately 2 weeks, OD_{660} reached a value above 5. If no growth was observed after two weeks, cultures were discarded. Each grown culture was restreaked on an SMD_{NO3} agar plate to yield single colonies. One single colony from each independent adaptation experiment was inoculated in 100 mL SMD_{NO3} and stored at −80 °C. Adaptation of strain IMX1781 resulted in independently evolved isolates IMS815, IMS816, and IMS819 while adaptation of IMX1782 resulted in evolved isolates IMS817, IMS818, and IMS821.

For the determination of the specific growth rates of evolved strains IMS815-819, IMS821, and of *O. parapolymorpha* DL-1 and *B. bruxellensis* CBS 2499, frozen stock cultures were used to inoculate 20 mL starter cultures. These were subsequently used to inoculate 100 mL SMD_{NO3} flask cultures to initial OD_{660} values between 0.1 and 0.2. Growth of these cultures was monitored with a 7200 Jenway Spectrophotometer (Jenway, Stone, United Kingdom). Specific growth rates were calculated from at least five time points in the exponential growth phase of each culture.

2.8. Anaerobic growth experiments

Anaerobic growth of the engineered *S. cerevisiae* strain IMS816 and

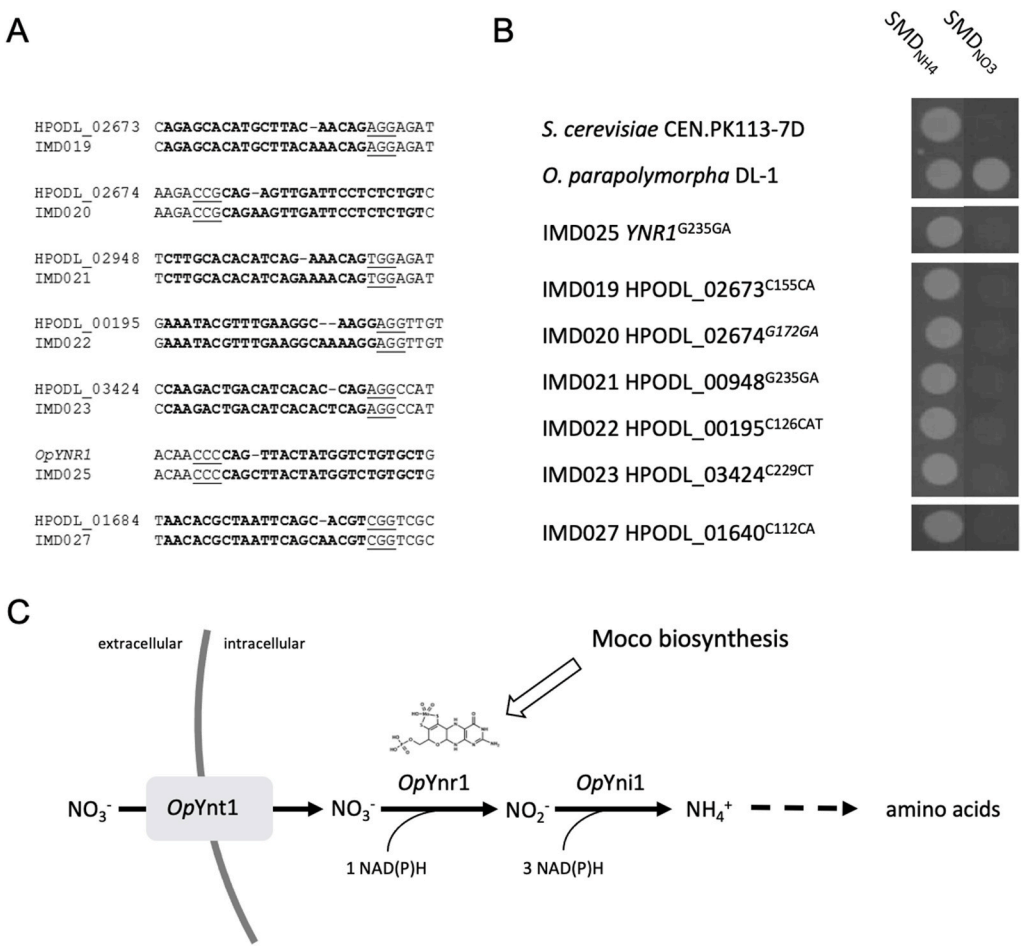

Fig. 2. Frameshift mutations in putative Moco biosynthesis genes impair nitrate assimilation in *O. parapoly morpha*. (A) Sanger-sequencing results showing the presence of -frameshift mutations in *O. parapolymorpha* strains after targeted *Spy*Cas9-directed double-strand breaks in candidate Moco biosynthesis genes. The 20 bp gRNA targeting sequences are shown in bold, PAM sequences are underlined. (B) Spot plate of the wild-type *O. parapolymorpha* and mutant strains on SMD with either ammonium (SMD_{NH4}) or nitrate (SMD_{NO3}) as sole nitrogen source. As a control, the NR *OpYNR1* gene encoding nitrate reductase was also targeted and mutated. Pictures were taken after 24 h incubation at 30 °C. All strains were spotted on the same agar plate and then re-arranged in the photograph. (C) Schematic representation of the nitrate assimilation pathway including a high-affinity nitrate transporter (*Op*Ynt1), a Moco-dependent NR (*Op*Ynr1), and a nitrite reductase (*Op*Yni1). The dashed line represents multiple enzyme-catalysed reactions.

the wild-type *B. bruxellensis* strain CBS 2499 was studied in a Lab Bactron 300 anaerobic workstation (Sheldon Manufacturing Inc., Cornelius, OR) containing an atmosphere of 85% N_2, 10% CO_2 and 5% H_2. Exponentially growing aerobic cultures were used to inoculate anaerobic starter cultures at a OD_{600} of about 0.2. These starter cultures were grown in 50-mL shake flasks containing 40 mL of SMD_{NO3} supplemented with 40 g/L glucose and used inoculate a second anaerobic culture on SMD_{NO3} with 20 g/L glucose. Anaerobic cultures were incubated at 30 °C and shaken at 240 rpm on an IKA KS 260 Basic orbital platform (Dijkstra Verenigde BV, Lelystad, The Netherlands). A regularly regenerated Pd catalyst for H_2-dependent oxygen removal was placed inside the anaerobic chamber. Optical density at 600 nm was periodically

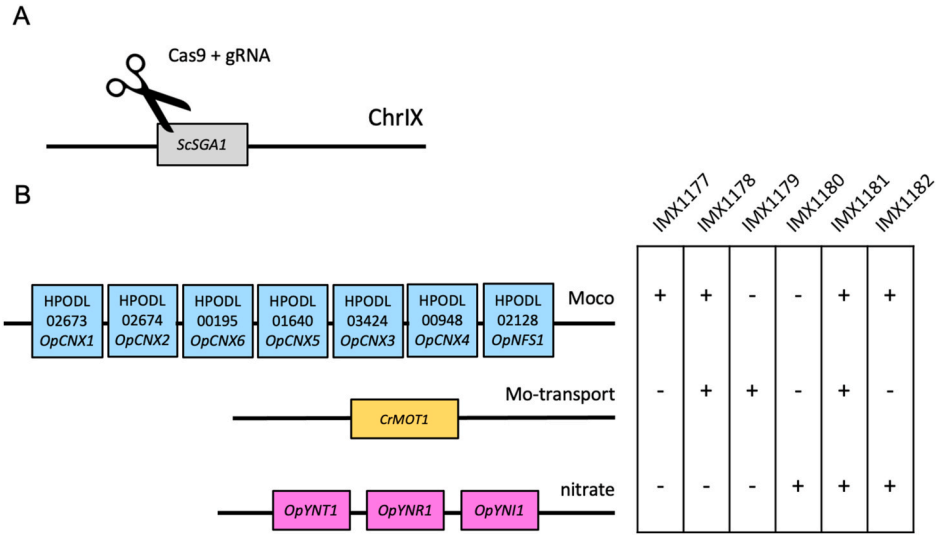

Fig. 3. Schematic overview of *S. cerevisiae* strain construction. All genes were integrated by CRISPR/Cas9 in one step at the *SGA1 locus* on chromosome IX (A). One or more of the moco, Mo-transport, and nitrate modules were integrated, resulting in strains IMX1177, IMX1178, IMX1179, IMX1180, IMX1181, and IMX1182 (B).

measured using a Ultrospec 10 spectrophotometer (Biochrom, Cambridge, United Kingdom). Sterile media was placed inside the anaerobic chamber at least 24 h prior to inoculation to ensure removal of residual oxygen. When indicated, SMD_{NO3} media were supplemented with 1 mL/L of a concentrated hemin solution that was prepared by adding 0.05% (w/v) hemin (Sigma Aldrich) to a 1:1 ethanol:water solution with 50 mM NaOH. As a negative control for oxygen leaks, a parallel culture of *S. cerevisiae* CEN. PK113-7D strain on SMD_{Urea} without the anaerobic growth factors Tween 80 and ergosterol was included in all anaerobic growth experiments (Dekker et al., 2019).

2.9. Competitive cultivation

Frozen stock cultures of *S. cerevisiae* strains IMX585 (*MATa SpyCas9*), IMS816 (Moco - Mo importer - Nitrate) and of *B. bruxellensis* CBS 2499 were used to inoculate 20 mL starter cultures, which were subsequently used to inoculate 100 mL flask cultures on SMD_{NO3}. Upon reaching mid-exponential phase ($1 < OD_{660} < 5$), these cultures were centrifuged at 3000 g for 5 min and washed three times in demineralized water. Cells were then resuspended in SMD_{NO3} and co-inoculated at an initial OD_{660} of 0.1 in 100 mL shake-flask cultures on SMD_{NO3}. Triplicate co-cultures were prepared for strain pairs IMX585/CBS 2499 and IMS816/CBS 2499. Flasks were incubated for 48 h prior to plating diluted samples on $SMD_{NO3\text{-}blue}$ and $SMD_{Amm\text{-}blue}$ plates. Plates were incubated for 4 days at 30 °C and then 2 weeks at 4 °C to develop bromocresol green staining prior to imaging and colony counting (Supplementary Fig. S7).

2.10. Whole-genome sequencing

Genomic DNA of strains IMX1781, IMX1782, IMS815, IMS816, IMS817, IMS818, and IMS821 was isolated with a Blood & Cell Culture DNA Kit with 100/G Genomics-tips (QIAGEN, Hilden, Germany) following manufacturer's instructions. Illumina-based paired-end sequencing with 150-bp reads was performed on 300-bp insert libraries (Novogene Company Limited, Hong Kong, China) with a minimum resulting coverage of 50 x. Data mapping was performed using bwa 0.7.15-r1142-dirty against the CEN. PK113-7D genome (Salazar et al., 2017) to which an extra contig containing the relevant integration cassette had been previously added. Data processing and chromosome copy number variation determinations were done as previously described (Nijkamp et al., 2012; Perli et al., 2020b).

2.11. In vitro nitrate reductase activity measurements from cell extract

Frozen stock cultures of *S. cerevisiae* strains IMX1780, IMX1781 and IMS816 were used to inoculate 20 mL starter cultures on SMD_{urea}, which were then used to inoculate 100-mL shake flask cultures on the same medium, to an initial OD_{660} of 0.2. Shake flasks were incubated for 24 or 48 h, until the OD_{660} exceeded 30. Cultures were then centrifuged at 3000 g for 5 min and supernatant was discarded. Lysis buffer was prepared by dissolving 1 tablet of complete ULTRA EDTA-free protease inhibitor cocktail (Roche, Basel, Switzerland) in 10 mL ice-cold 100 mM potassium phosphate buffer (pH 7). Cell pellets were resuspended in 1.5 mL lysis buffer and transferred to 1.5 mL bead-beating tubes along with 0.75 *g* of 400–600 μm acid-washed glass beads (Sigma Aldrich) per tube. Cells were disrupted by six 1-min cycles at 5 m/s speed in a Fast-Prep 24 cell homogenizer (MP Biomedicals, Santa Ana, CA), with 5-min cooling on ice between cycles. Samples were then centrifuged at 14000 *g* and at 4 °C for 10 min. Supernatant was collected in 10 mL centrifuge tubes, diluted by adding 2 mL ice-cold lysis buffer and centrifuged at 20000 *g* and at 4 °C for 1 h. Clear supernatant were then transferred into clean 15 mL plastic tubes and kept on ice prior to analysis. Nitrate-reductase activity was measured by monitoring either NADH or NADPH consumption at 340 nm using a spectrophotometer (Jasco, Easton, MA). Reactions were performed at 30 °C, in 100 mM phosphate buffer pH7. Reaction mixtures included 20 μM FAD, and either 50 or 100 μl of clarified cell extract. After addition of 200 μM NADH or NADPH, background activity was monitored, after which 0.005, 0.05, 1 or 2 mM KNO_3 was added to initiate the reaction. Reaction rates were corrected based on an extinction coefficient of NADH and NADPH of 6.22 mM^{-1} cm^{-1} at 340 nm and corrected for the background activity in the absence of nitrate. Protein contents of cell extracts were quantified with a Quick Start Bradford Assay (Bio-Rad Laboratories, Hercules, CA) following manufacturer's instructions. Specific activities of nitrate reductase in cell extracts were expressed in μmol $NAD(P)^+$ min^{-1} (mg protein).$^{-1}$

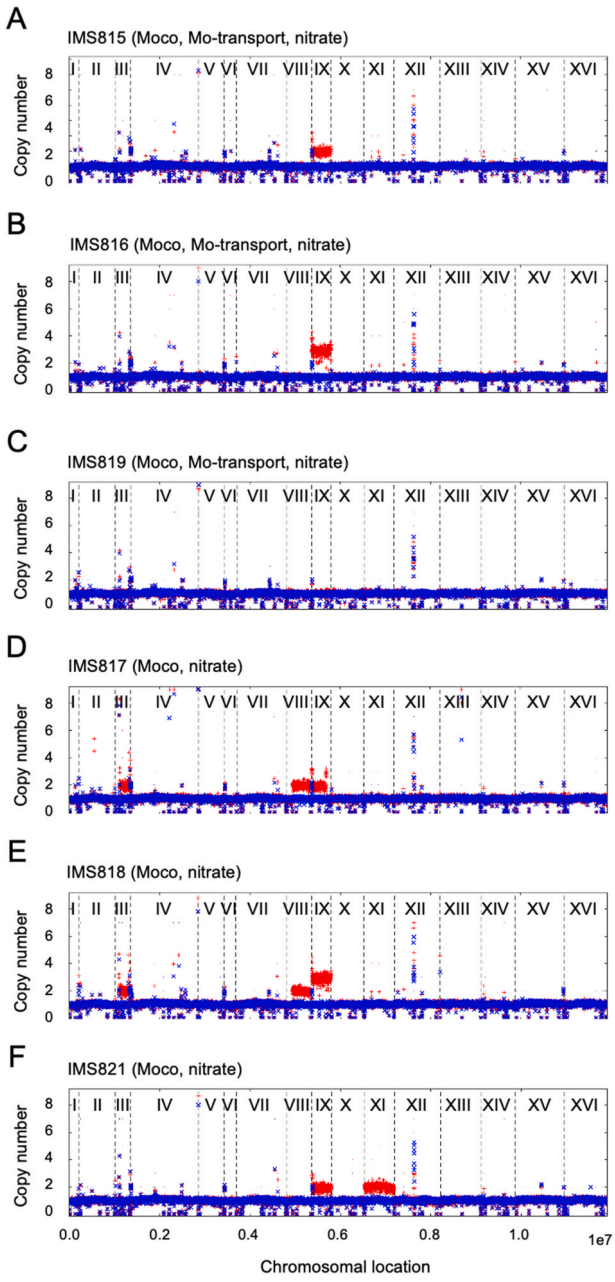

Fig. 4. Chromosomal copy number variations in engineered *S. cerevisiae* strains evolved for growth in SMD with 50 mM KNO_3 as sole nitrogen source. Strains *S. cerevisiae* IMS815 (A), IMS816 (B) and IMS819 (C) were evolved starting from strain IMX1781 (Moco, Mo-transport, nitrate) while strains IMS817 (D), IMS818 (E) and IMS821 (F) were evolved starting from strain IMX1782 (Moco, nitrate). Copy numbers of chromosomes and chromosomal regions were calculated from sequence data with the Magnolya algorithm (Nijkamp et al., 2012). Results for the parental unevolved strain and the evolved isolate are shown in blue and red, respectively. Individual chromosomes are indicated by Roman numerals and separated by dashed lines.

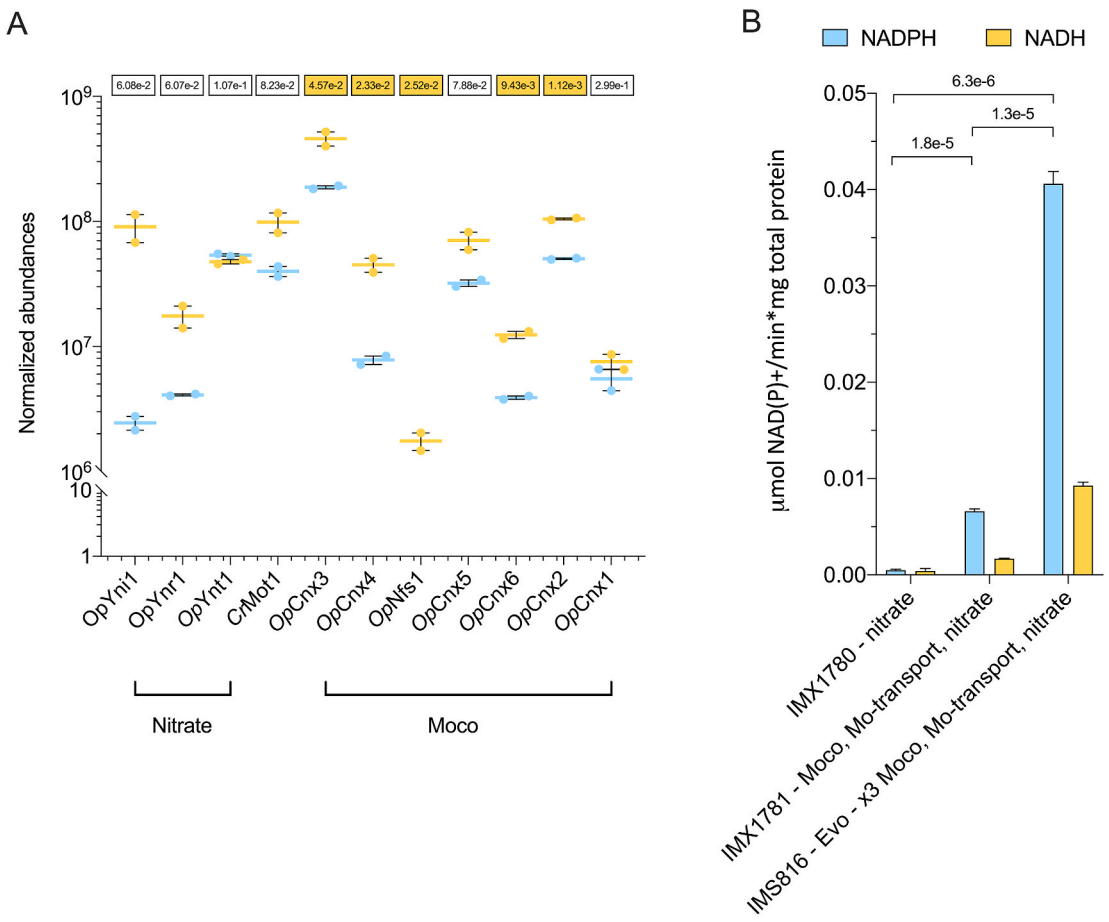

Fig. 5. Evolved nitrate-assimilating *S. cerevisiae* strains show increased Moco biosynthesis and nitrate-assimilation protein expression levels and higher *in vitro* nitrate-reductase activity. (A) Normalized abundances of heterologously expressed proteins in strains IMX1781(Moco, nitrate, Mo-transport, light blue) and IMS816 (Evolved IMX1781, ×3 Moco, ×3 nitrate, ×3 Mo-transport, yellow) measured by LC-MS. P-values from a two-tailed Welch's *t*-test are shown above each tested pair and highlighted in yellow when P-value < 0.05. (B) Nitrate reductase activity in cell extracts derived from overnight cultures of IMX1780 (nitrate), IMX1781 (Moco, nitrate, Mo-transport), and IMS816 (Evolved IMX1781, ×3 Moco, ×3 nitrate, ×3 Mo-transport) grown on SMD_{urea}. Statistical analysis was based on a two-tailed Welch's *t*-test and P-values are reported for tested pairs. Error bars represent the standard error of the mean of biological replicates (n = 2 for panel A, n = 3 for panel B).

2.12. Proteome analysis

Starter cultures on 20 mL SMD_{urea} were inoculated with frozen stock cultures of strains IMX1781 and IMS816 and used to inoculate two independent 100 mL flask cultures for each strain at an initial OD_{660} of 0.2. Once these cultures reached and OD_{660} of 4, 1 mL broth was collected and centrifuged at 3000 g for 5 min. The cell pellet, which had a volume approximately 60 µl was then subjected to protein extraction and trypsin digestion (Boonekamp et al., 2020). Prior to analysis, peptides were resuspended in 30 µl of 3% acetonitrile/0.01% trifluoroacetic acid and peptide concentrations were measured with a Nanodrop spectrophotometer (Thermo Scientific) set at 280 nm. One µg of sample was injected into a CapLC system (Thermo Scientific) coupled to an Orbitrap Q-exactive HF-X mass spectrometer (Thermo Scientific). After capture of samples, at a flow rate of 10 µL/min on a precolumn (µ-precolumn C18 PepMap 100, 5 µm, 100 Å), peptides were separated on a 15-cm C18 easy spray column (PepMap RSLC C18 2 µm, 100 Å, 150 µmx15cm) at a flow rate of 1.2 µL/min and with a 60-min continuous gradient from 4% to 76% acetonitrile in water. Data analysis was performed using Proteome discover 2.4 (Thermo Scientific) with fixed modifications set to carbamidomethyl (C), variable modifications set to oxidation of methionine residues, search mass tolerance set to 20 ppm, MS/MS tolerance set to 20 ppm, trypsin selected as hydrolytic enzyme and allowing one missed cleavage. False discovery rate was set at 0.1% and the match between runs window was set to 0.7 min. Quantification was exclusively based on unique peptides and normalization between samples was based on total peptide amount. A protein database consisting of the *S. cerevisiae* S288c proteome amino-acid sequences together with sequences of the heterologously expressed proteins was used for protein searches. For each strain analyses were performed on independent biological duplicate samples.

2.13. Analytical methods

Metabolite concentrations in culture supernatants were analysed by high-performance liquid chromatography (HPLC) on an Agilent 1260 HPLC (Agilent Technologies, Santa Clara, CA) fitted with a Bio-Rad HPX 87 H column (Bio-Rad). The flow rate was set at 0.6 mL min^{-1}, 0.5 g L^{-1} H_2SO_4 was used as eluent and the column temperature was 65 °C. An Agilent refractive-index detector and an Agilent 1260 VWD detector were used for metabolite quantification (Verhoeven et al., 2017). Nitrate, nitrite and ammonium concentrations culture supernatants were measured with a Hach DR3900 spectrophotometer and Hach kits LCK 339, LCK 341, and LCK 304 (Hach Lange, Düsseldorf, Germany), according to the manufacturer's instructions.

2.14. Statistical analysis

Statistical significance of differences between measurements from replicate cultures were calculated by using a two-tailed *t*-test assuming

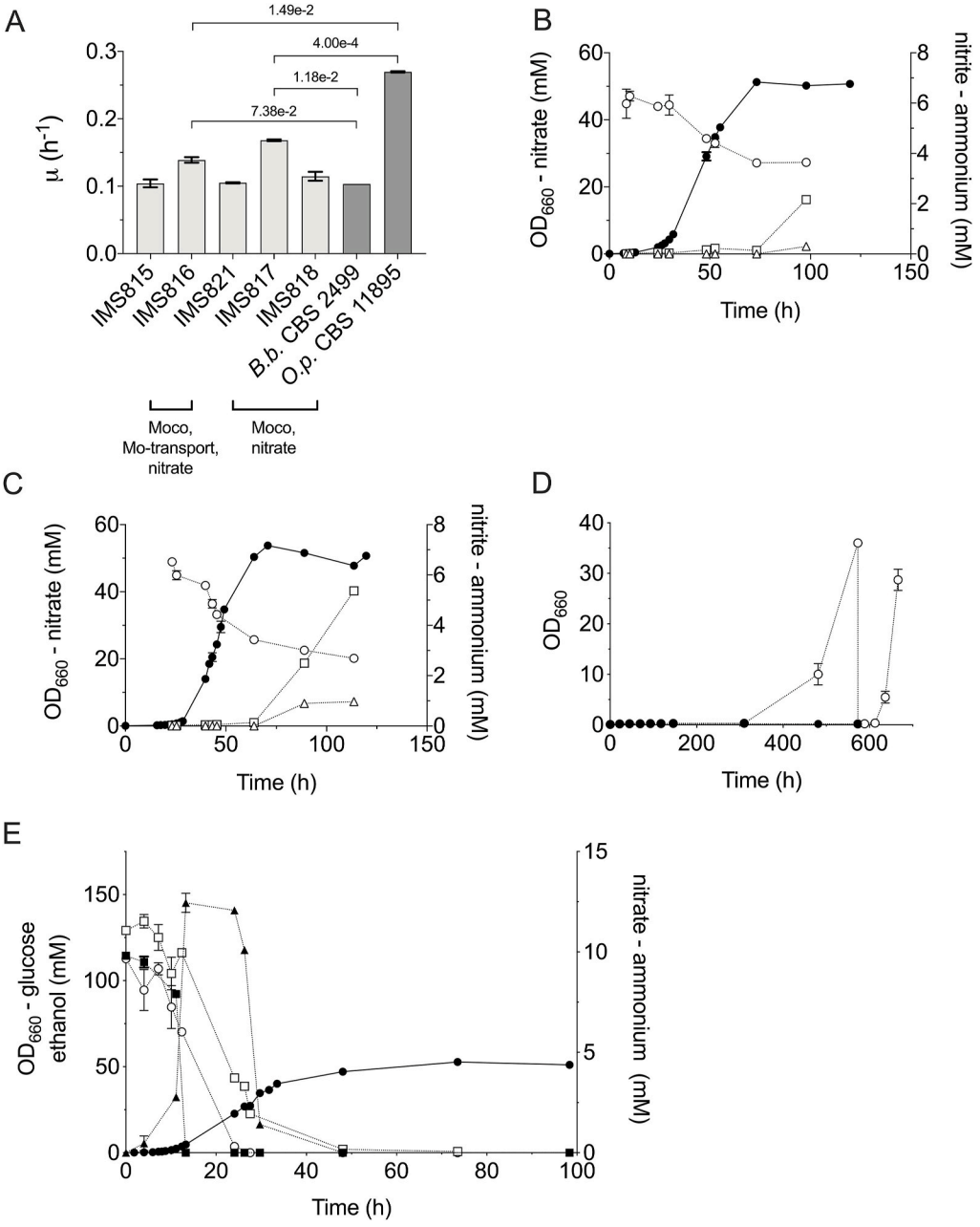

Fig. 6. Aerobic characterization of engineered and evolved nitrate-assimilating *S. cerevisiae* strains. (A) Specific growth rates in aerobic shake-flask cultures of evolved *S. cerevisiae* strains IMS815, IMS816, IMS817, IMS818, IMS821, *B. bruxellensis* CBS 2499, and *O. parapolymorpha* CBS 11895 on SMD_{NO3}. Growth curves of aerobic shake-flask cultures of *S. cerevisiae* strains IMS816 (Evolved IMX1781, ×3 Moco, ×3 nitrate, ×3 Mo-transport, B) and IMS817 (Evolved IMX1782, ×2 Moco, ×2 nitrate, C) in SMD_{NO3}. Symbols indicate biomass (●) and nitrate (○), nitrite (□) and ammonium (△). (D) Growth curves of IMS816 (Evolved IMX1781, ×3 Moco, ×3 nitrate, ×3 Mo-transport, ○) and IMS817 (Evolved IMX1782, ×2 Moco, ×2 nitrate, ●) in $SMD_{NO3\text{-}LowMo}$ containing 16 nM MoO_4^{2-}. (E) Growth curve in aerobic shake-flask cultures of *S. cerevisiae* IMS817 (Evolved IMX1782, ×2 Moco, ×2 nitrate) on SMD_{AN} containing 10 mM NH_4NO_3 as nitrogen source. Symbols indicate OD_{660} (●), glucose (■), ethanol (▲), ammonium (○), and nitrate (□). Statistical analysis was based on a two-tailed Welch's *t*-test and P-values are reported for tested pairs. Error bars represent the standard error of the mean of independent cultures (n = 3 except for panel D and CBS 2499, and CBS 11895 in panel A where n = 2).

unequal variances (Welch's correction).

2.15. Data availability

All measurement data and calculations used to prepare Figs. 2–7 and Supplementary Figs. S7–8 of the manuscript are available at the 4TU. Centre for research data repository (https://researchdata.4tu.nl/) under https://doi.org/10.4121/13194518. DNA sequencing data of *Saccharomyces cerevisiae* strains IMX1781-2, IMS815-19, and IMS821 were deposited at NCBI (https://www.ncbi.nlm.nih.gov/) under BioProject accession number PRJNA658462. Mass spectrometry proteomics data have been deposited to the ProteomeXchange Consortium (http://www.proteomexchange.org/) via the PRIDE partner repository with the dataset identifier PXD020472.

3. Results

3.1. Identification of moco biosynthesis genes in O. parapolymorpha

As a nitrate-assimilating yeast, *O. parapolymorpha* DL-1 can express a functional nitrate reductase (NR). Its genome should therefore carry a full complement of Moco biosynthesis genes, but these have not yet been annotated or characterized. A tBLASTn search of *O. parapolymorpha* DL-1 transcriptome data (Ravin et al., 2013) for orthologs of seven *E. coli* Moco biosynthesis genes yielded strong hits (E value < $1.0e^{-14}$) with six queries (Fig. 1, Table 4). A seventh, MoaD, yielded only a weak hit (E-value score 1.4 and 23.5% sequence identity; Supplementary Table S1) with transcript HPODL_03424 (CnxE). However, *Ec*MogA and *Ec*MoeA showed strong similarities with the 5′ and 3′ ends, respectively, of the same coding sequence. This observation indicated that, similar to the situation in other eukaryotes, a single *O. parapolymorpha* protein carries MPT adenylyltransferase and molybdenumtransferase domains

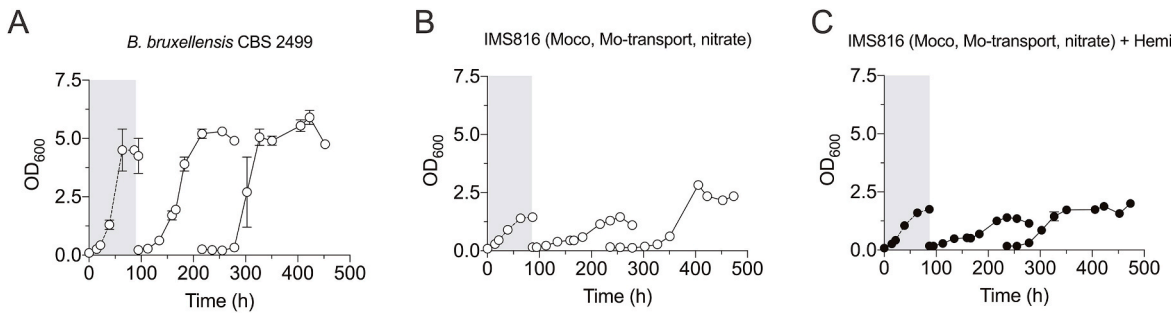

Fig. 7. Anaerobic growth of the engineered and evolved nitrate-assimilating *S. cerevisiae* strain IMS816 and *B. bruxellensis* CBS2499 on glucose synthetic medium with nitrate as sole nitrogen source. Strain CBS 2499 (A) and IMS816 (Evolved IMX1781, ×3 Moco, ×3 nitrate, ×3 Mo-transport, B–C) were sequentially transferred in SMD_{NO3} supplemented with Tween 80 and ergosterol with (●) or without (○) addition of hemin. A first anaerobic batch-cultivation cycle to deplete possible heme *b* introduced with the aerobically pre-grown inoculum is highlighted by a grey box. The absence of oxygen leaks in the anaerobic chamber was verified by near-absence of growth of *S. cerevisiae* CEN. PK113-7D on SMD_{Urea} without supplementation of the anaerobic growth factors Tween 80 and ergosterol (Supplementary Fig. S7). Error bars represent the standard error of the mean of independent cultures (n = 2).

Table 4
tBLASTn analysis of *E. coli* Moco-biosynthesis-related proteins versus *O. parapolymorpha* transcriptome.

Query protein (Uniprot ID)	Protein annotation	Filamentous fungi ortholog gene name	Gene name of first hit in O. parapolymorpha (E value - % query cover)	Proposed yeast gene name
***E. coli* MoaA (P30745)**	GTP 3′,8-cyclase	*cnxA*	HPODL_02673 ($5e^{-64}$ - 93)	*OpCNX1*
***E. coli* MoaC (P0A738)**	Cyclic pyranopterin monophosphate synthase	*cnxB*	HPODL_02674 ($1e^{-39}$ - 87)	*OpCNX2*
***E. coli* MoeB (P12282)**	Molybdopterin-synthase adenylyltransferase	*cnxF*	HPODL_00948 ($7e^{-50}$ - 97)	*OpCNX4*
***E. coli* IscS (P0A6B7)**	Cysteine desulfurase	*NFS1*	HPODL_02128 ($3e^{-172}$ - 99)	*OpNFS1*
***E. coli* MoaD (P30748)**	Molybdopterin synthase sulfur carrier subunit	*cnxG*	HPODL_01640 (1.4–95)	*OpCNX5*
***E. coli* MoaE (P30749)**	Molybdopterin synthase catalytic subunit	*cnxH*	HPODL_00195 ($4e^{-15}$ - 72)	*OpCNX6*
***E. coli* MogA (P0AF03)**	Molybdopterin adenylyltransferase	*cnxE (E)*	HPODL_03424 ($4e^{-21}$ - 76)	*OpCNX3*

(Llamas et al., 2004; Llamas et al., 2006).

The six identified coding sequences were manually annotated in the *O. parapolymorpha* genome sequence (PRJNA60503) and checked for presence of alternative in-frame start codons. *Ec*MoaA (GTP 3′,8-cyclase) orthologs such as human MOCS1A and *Arabidopsis thaliana* Cnx2 are known to be iron-sulfur cluster proteins that localize to the mitochondria (Marelja et al., 2008; Teschner et al., 2010). Sequence analysis of the *Ec*MoaA ortholog HPODL_02673 (CnxA) indicated that an N-terminal mitochondrial signal peptide sequence had been missed in the original annotation.

Individual disruption mutants of six of the *O. parapolymorpha* candidate genes (HPODL_02673, HPODL_02674, HPODL_00948, HPODL_01640, HPODL_00195, and HPODL_03424) were successfully constructed by introducing frameshifts within the first 30% of each coding sequence with *Spy*Cas9 (Fig. 2A). Attempts to disrupt of HPODL_02128 (*OpNFS1*) were not successful, suggesting that, as in *S. cerevisiae*, *Op*Nfs1 is essential due to its roles in iron-sulfur cluster biosynthesis and tRNA thiolation (Giaever et al., 2002). The ability of disruption mutants to use nitrate as sole nitrogen source was tested by spot-plate assays (Fig. 2B). The *S. cerevisiae* reference strain CEN. PK113-7D and the *O. parapolymorpha* DL-1 reference strains, as well as the NR-deficient *O. parapolymorpha* strain IMD025 (*OpYNR1*^{G235GA}) were included as controls. As expected, the DL-1 strain, but not strains CEN. PK113-7D and IMD025 grew on SMD_{NO3}. Consistent with involvement of the six candidate genes in Moco synthesis, the corresponding *O. parapolymorpha* disruption mutants (IMD019, IMD020, IMD021, IMD022, IMD023, and IMD027) did not grow on SMD_{NO3} (Fig. 2C).

3.2. Design of Moco biosynthesis and nitrate assimilation in S. cerevisiae

Since *S. cerevisiae* does not naturally express molybdenum-dependent enzymes, Moco synthesis by this yeast may not only require functional expression of Moco biosynthesis genes, but also of a molybdate transporter. Heterologous genes required for Moco biosynthesis and nitrate assimilation were therefore grouped in three functional modules (1) Moco biosynthesis (Moco) comprising HPODL_02128 (*OpNFS1*), HPODL_02673 (*OpCNX1*), HPODL_02674 (*OpCNX2*), HPODL_00948 (*OpCNX4*), HPODL_01640 (*OpCNX5*), HPODL_00195 (*OpCNX6*), and HPODL_03424 (*OpCNX3*), (2) Molybdate high-affinity transport (Mo-transport) consisting of *CrMOT1* from the unicellular green alga *Chlamydomonas reinhardtii* (Tejada-Jimenez et al., 2007) and (3) Nitrate assimilation (nitrate) comprising of *O. parapolymorpha* genes encoding a high-affinity nitrate transporter (*OpYNT1*), nitrate reductase (*OpYNR1*), and nitrite reductase (*OpYNI1*). Theoretically, an engineered *S. cerevisiae* strain expressing these three modules should be able to grow with nitrate as the sole nitrogen source. Although *S. cerevisiae* has a native *NFS1* gene, *Sc*Nfs1 predominantly localizes to the mitochondria (Kispal et al., 1999). In contrast, human Nfs1 contributes to Moco biosynthesis in the cytosol (Marelja et al., 2013). To ensure a sufficient activity of Nfs1 in the cytosol of *S. cerevisiae*, *OpNFS1* was included in the Moco module. Each module was integrated individually or in combination with other modules at the *SGA1* locus on chromosome IX in one single transformation (Fig. 3A). This genomic locus has been previously shown to be a suitable integration site for single or multiple genes expression modules (Kuijpers et al., 2016; Mans et al., 2015).

3.3. Growth of S. cerevisiae on nitrate required amplification of the Moco biosynthesis and nitrate assimilation pathway genes

Transformation of the different modules resulted in *S. cerevisiae* strains IMX1777 (Moco), IMX1778 (Moco, Mo-transport), IMX1779 (Mo-transport), IMX1780 (nitrate), IMX1781 (Moco, Mo-transport, nitrate) and IMX1782 (Moco, nitrate) (Fig. 3B, Figs. S1–6). After a short adaptive laboratory evolution of two weeks, only strains IMX1781 (Moco, Mo-transport, nitrate) and IMX1782 (Moco, nitrate) grew on synthetic medium with nitrate, indicating that next to adaptation,

expression of the Moco and nitrate modules was essential for nitrate assimilation, while, under these conditions, high-affinity Mo-transport was dispensable.

To further investigate the genetic basis of this adaptation, evolved populations derived from IMX1781 and IMX1782 were each inoculated in triplicate shake-flask cultures on SM_{NO3}. After reaching stationary phase, single-colony isolates were obtained from these cultures and named IMS815-6, and IMS819 (derived from IMX1781), and IMS817-8, and IMS821 (derived from IMX1782). Whole-genome sequencing showed a disomy or trisomy of chromosome IX, which harboured the *SGA1* locus at which the heterologous genes were integrated (Fig. 4), in five of these six isolates. This change in chromosomal copy number was not observed in a culture of the parental strains IMX1781 and IMX1782 grown on complex YPD medium. Strain IMS819, which did not show aneuploidy, but had lost mitochondrial DNA and was therefore not used in further experiments because of its inability to respire.

To assess the impact of the observed changes in copy number of chromosome IX on expression levels of the heterologous proteins, strain IMX1781, which contains all three modules (Moco, Mo-transport, nitrate) and the derived isolate IMS816 were analysed by untargeted proteomics (Fig. 5A). The heterologously expressed proteins were all detected in both strains, except for *Op*Nfs1 which was not detected in the unevolved strain IMX1781 (Moco, Mo-transport, nitrate). Statistical analysis of normalized peptide counts showed that levels of five Moco biosynthetic proteins (*Op*Cnx2, *Op*Cnx3, *Op*Cnx4, *Op*Cnx6, and *Op*Nfs1) were significantly higher (P-value < 0.05) in the evolved isolate IMS816 than in the parental strain IMX1781.

NADPH- and NADH-dependent NR activity was assayed in cell extracts of strains IMX1780 (nitrate), IMX1781 (Moco, Mo-transport, nitrate), and IMS816 (evolved IMX1781) (Fig. 5B). Cell extracts of strain IMX1780, which lacks the Moco module, showed no significant NR activity with either redox cofactor. In contrast, extracts from strains IMX1781 and IMS816 both showed NR activity, with a ca. 5-fold increased activity in the latter strain. Activities observed with NADPH as electron donor were approximately four-fold higher than with NADH. These results indicate that strain IMX1781 already expressed a functional nitrate assimilation pathway and that its cultivation SM_{NO3} provided a strong selective pressure for amplification of the heterologous gene cassettes, leading to increased protein expression and enzyme capacity.

3.4. Growth characteristics of engineered nitrate-assimilating *S. cerevisiae*

Specific growth rates of the evolved *S. cerevisiae* isolates IMS815-8 and IMS821 measured in shake-flask cultures on SMD_{NO3} ranged from 0.10 to 0.17 h^{-1} (Fig. 6A). These specific growth rates are two-to three-fold lower than that of a congenic reference strain on SMD with ammonium as nitrogen source (Perli et al., 2020a). Compared to natural nitrate-assimilating yeasts, *S. cerevisiae* strains IMS816 and IMS817 grew faster than *B. bruxellensis* CBS 2499 (specific growth rate of 0.1 h^{-1} on SMD_{NO3}) but up to 2.5-fold slower than *O. parapolymorpha* CBS 11895 (specific growth rate of 0.25 h^{-1} on SMD_{NO3}). During exponential growth on SMD_{NO3}, nitrate consumption by fastest growing nitrate-assimilating *S. cerevisiae* strains IMS816 (evolved IMX1781, Moco, Mo-transport, nitrate) IMS817 (evolved IMX1782, Moco, nitrate) occurred without detectable accumulation of either nitrite or ammonium (Fig. 6B and C). Release of small amounts of ammonium in late stationary phase cultures was tentatively attributed to protein turnover and/or cell lysis.

To test whether expression of a high-affinity Mo-transporter was essential at low extracellular molybdate concentrations, strains IMS816 and IMS817 were inoculated in SMD_{NO3} with a 100-fold lower MoO_4^{2-} concentration than the reference medium (16 nM instead of 1.6 μM, Fig. 6D). After two weeks of incubation, only strain IMS816 started growing on the low-molybate medium and, upon transfer to the same medium, instantaneously grew exponentially at a rate of 0.11 ± 0.01 h^{-1}. This observation indicated that, after an adaptation period, the Mo-transport module was required for growth at low molybdate concentrations.

The ability of strain IMS817 (Moco, nitrate) to co-consume nitrate and ammonium was tested in shake-flask cultures on SMD_{AN}, which contained 10 mM NH_4NO_3 as nitrogen source (Fig. 6E). Although ammonium and nitrate were consumed at different rates, nitrate and ammonium were consumed simultaneously. Nitrate was completely consumed (residual concentration < 0.1 mM) and a high specific growth

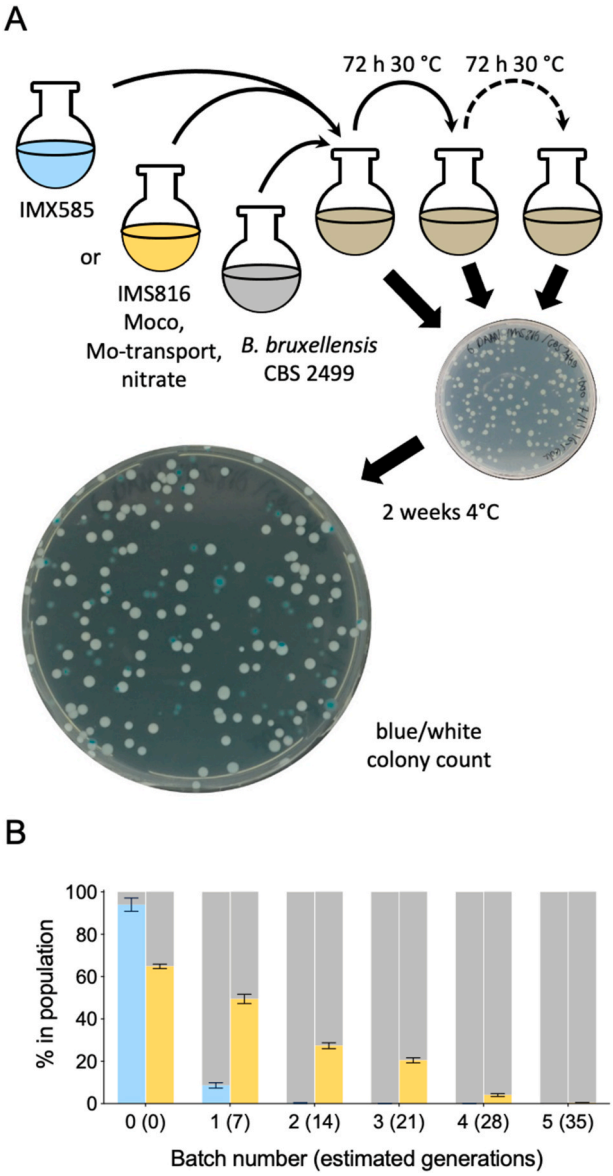

Fig. 8. The engineered nitrogen-assimilating *S. cerevisiae* strain IMS816 shows increased competitiveness in co-cultures with the spoilage yeast *B. bruxellensis*. (A) Schematic representation of the co-cultivation experiment. Either the reference strain *S. cerevisiae* IMX585 (light blue) or strain IMS816 (Evolved IMX1781, ×3 Moco, ×3 nitrate, ×3 Mo-transport, yellow) was co-inoculated with *B. bruxellensis* CBS 2499 (grey) and grown in serial batch cultures. Before each transfer, cells were plated on both $SMD_{NO3\text{-}blue}$ and $SMD_{Amm\text{-}blue}$ agar plates. After 48 h at 30 °C, followed by 2 weeks at 4 °C to selectively stain CBS 2499 colonies, *S. cerevisiae* (white) and *B. bruxellensis* (blue) colonies were counted. (B) Development over time of the percentage of IMX585 (light blue) or IMS816 (Evolved IMX1781, ×3 Moco, ×3 nitrate, ×3 Mo-transport, yellow) *S. cerevisiae* cells relative to total cell count (grey) of co-cultures with *B. bruxellensis* CBS 2499. Error bars represent the standard error of the mean of independent co-cultures (n = 3).

rate ($0.30 \pm 0.01\ h^{-1}$) was observed throughout the exponential growth phase.

In addition to Moco, NR requires a flavin adenine dinucleotide and heme *b* as cofactors (Campbell, 1999; Guerrero et al., 1981). In *S. cerevisiae*, heme *b* is synthesized via an oxygen-dependent pathway (Camadro et al., 1994; Zagorec et al., 1988). To test whether the nitrate-assimilating *S. cerevisiae* strain IMS816 (Moco, Mo-transport, nitrate, evolved) was nevertheless able to assimilate nitrate under anaerobic condition, its growth on SMD_{NO3} was studied in an anaerobic chamber. The wild-type *B. bruxellensis* strain CBS 2499, which was previously reported to grow anaerobically on nitrate (Pena-Moreno et al., 2019) was included as a reference. Although *B. bruxellensis* CBS 2499 reproducibly showed anaerobic growth after three consecutive transfers in SMD_{NO3}, the cultures reached only low OD values. *S. cerevisiae* strain IMS816 grew slower and reached final OD values that were over two-fold lower than those observed in anaerobic cultures of *B. bruxellensis* CBS 2499 (Fig. 7A and B). Supplementation of 32 mg/L of hemin (Fe^{3+}-containing protoporphyrin IX), which can be imported by *S. cerevisiae* when grown anaerobically (Protchenko et al., 2008), did not result in faster anaerobic growth of strain IMS816 on SMD_{NO3} (Fig. 7C). This result indicates that the heme *b* is not the only limiting factor in the tested conditions and time frames (Protchenko et al., 2008).

3.5. Competition of nitrate-assimilating *S. cerevisiae* and the spoilage yeast- *B. bruxellensis* in nitrate-containing media

B. bruxellensis strains are common yeast contaminants in bioethanol plants (Abbott et al., 2005; da Silva et al., 2016; de Souza Liberal et al., 2007). Their spoilage phenotype has been related to utilization of nutrients in industrial media that cannot be metabolized by *S. cerevisiae* (Crauwels et al., 2015; Parente et al., 2018). Plant biomass-derived substrates, such as the sugarcane juice used in Brazilian bioethanol processes, contains nitrate (de Barros Pita et al., 2011). In such settings, the ability to (co-)consume nitrate may confer a competitive advantage with *S. cerevisiae* (de Barros Pita et al., 2011). To evaluate the relative fitness of the engineered nitrate-assimilating *S. cerevisiae* strain IMS816 and *B. bruxellensis* CBS 2499, they were co-cultured in serial aerobic batch cultures on SMD_{NO3}. After inoculation at a *S. cerevisiae*: *B. bruxellensis* ratio of at least 6:4, based on the colonies ratios at time 0, cultures were sequentially transferred to fresh medium at 72 h intervals. As a control, a similar experiment was performed starting with a 9:1 mixture of the nitrate-non-assimilating reference strain *S. cerevisiae* IMX585 and *B. bruxellensis* CBS 2499. At the onset of each cultivation cycle, samples were plated on SMD with either ammonium or nitrate as nitrogen source, using Bromocresol Green for differential staining of the two species (Fig. 8A). In the control cultures, the relative abundance of *S. cerevisiae* IMX585 dropped below 10% after the first cultivation cycle and below detection level after the second transfer. In contrast, in a co-culture of the nitrate-assimilating *S. cerevisiae* strain IMS816 and *B. bruxellensis* CBS 2499, the *S. cerevisiae* strain persisted in the co-culture for about 35 generations (Fig. 8B).

4. Discussion

Over 50 molybdenum-cofactor (Moco) containing enzymes, mostly from prokaryotes, have been characterized and catalyse redox reactions in the global cycles of nitrogen (e.g. nitrate reductase, nitrite oxidase), sulfur (e.g. sulfite oxidase, DMSO-reductase) and carbon (e.g. CO dehydrogenase, aldehyde oxidases, formate dehydrogenase) (Leimkuhler and Iobbi-Nivol, 2016). More molybdo-enzymes are likely to be discovered as part of the ongoing exploration of microbial diversity. Synthesis of a functional Moco in *S. cerevisiae* represents an essential step towards accessing this diverse group of enzymes for metabolic engineering strategies in this platform organism. In addition to the use of nitrate as a nitrogen source, such strategies could, for example, involve high-k_{cat} molybdoprotein formate dehydrogenase (Maia et al., 2015) as alternative for the low-k_{cat} native fungal formate dehydrogenases and molyboprotein furoyl-CoA dehydrogenase, which can contribute to conversion of furanic compounds found in lignocellulosic hydrolysates (Wierckx et al., 2011). Full exploration of these possibilities will require expansion of the range of Moco variants that can be expressed by *S. cerevisiae*.

Recent genome sequence based phylogeny studies showed that fewer than 27% of the 329 sequenced Saccharomycotina yeast species genomes harbour Moco biosynthesis genes and that only 13% harbour nitrate-reductase genes (Shen et al., 2018). The exact gene complement required for Moco synthesis in yeasts and other organisms has not previously been defined. The gene set identified in this study, based on a combination of mutational analysis in *O. parapolymorpha* and heterologous expression in *S. cerevisiae*, provides a basis for further investigation and engineering of fungal Moco biosynthesis. In this context, subcellular compartmentation of Moco synthesis deserves special attention. In eukaryotes, the molybdopterin biosynthesis intermediate cyclic pyranopterin monophosphate (cPMP) is synthesized in the mitochondrial matrix (Leimkuhler et al., 2017) (Fig. 1) and subsequently translocated to the cytosol for further processing. In *Arabidopsis thaliana*, *At*Atm3, a mitochondrial transporter involved in Fe–S cluster translocation (Schaedler et al., 2014), has been proposed to also transport cPMP (Teschner et al., 2010). *In vitro* and *in vivo* functionality of nitrate reductase in engineered strains suggests that *S. cerevisiae* can export cPMP from mitochondria. By analogy to the situation in *A. thaliana*, the mitochondrial ATP-binding cassette (ABC) transporter *Sc*Atm1, which is involved in transport of iron-sulfur (Fe/S) clusters precursors to the cytosol and essential for aerobic growth (Kispal et al., 1997; Leighton and Schatz, 1995), is a promising candidate for this role.

Despite the use of strong promoters to drive expression of *O. parapolymorpha* nitrate-assimilation and Moco-biosynthesis genes, growth of engineered *S. cerevisiae* strains on nitrate as sole nitrogen source reproducibly selected for mutants in which single-chromosome disomy or trisomy caused increased copy numbers of these genes. These increased copy numbers coincided with higher abundances of all encoded heterologous proteins (Fig. 4). Consequently, it is not possible to unequivocally identify which protein(s) exerted the strongest control on *in vivo* rates of nitrate reduction. However, only HPODL_02128 (OpNfs1) was not detected prior to gene amplification and may therefore be a priority target in follow-up research. Nfs1 is a cysteine desulfurase involved in iron-sulfur cluster (Fe/S) biogenesis and, in *S. cerevisiae*, is almost exclusively located in the mitochondria (Kispal et al., 1999). In *O. parapolymorpha*, cytosolic Nfs1 is also required to re-load sulfur on the molybdopterin-synthase adenylyltransferase *Op*Cnx4 (HPODL_00948) via a sulfur mobilization route shared with tRNA thiolation (Leimkuhler et al., 2017; Marelja et al., 2008, 2013).

Earlier reports proposed *S. cerevisiae* as a platform for molybdate import studies due to absence of native high-affinity molybdate transporters (Tejada-Jimenez et al., 2007). Our results show that, although it does not naturally express molybdoproteins, *S. cerevisiae* can take up MoO_4^{2-} at micromolar concentrations. A hypothesis that molybdate is transported by the sulfate transporters Sul1 and Sul2 was supported by the observation that expression of the plant sulfate transporter SHST1 enabled high-affinity molybdate import in *S. cerevisiae* (Deves and Boyd, 1989; Fitzpatrick et al., 2008). The demonstration that expression of a heterologous high-affinity transporter is required for growth at nM concentrations of molybdate may be relevant for application of Moco-expressing strains in feedstocks that contain extremely low molybdate concentrations.

After an earlier unsuccessful attempt to express a *Nicotiana tabacum* nitrate reductase (Truong et al., 1991), this study is the first to demonstrate nitrate assimilation by an engineered *S. cerevisiae* strain. In contrast to most naturally nitrate-assimilating fungi (de Barros Pita et al., 2013; Facklam and Marzluf, 1978; Siverio, 2002), the engineered nitrate-assimilating *S. cerevisiae* strains did not exhibit ammonium repression of nitrate assimilation and co-consumed both nitrogen

sources during fast aerobic growth on an ammonium-nitrate mixture. Hydrolysates of corn, corn stover and switchgrass used as feedstocks for yeast-based bioethanol production contain low but significant amounts of nitrate, whose discharge can have negative environmental consequences (Costello et al., 2009). The low rates of nitrate consumption by anaerobic cultures of nitrate-assimilating *S. cerevisiae* strains described in this study may already suffice to eliminate small amounts of nitrate and thereby contribute process sustainability. For more extensive use of nitrate as a nitrogen source in anaerobic bioethanol production processes, for instance to reoxidize cytosolic NADH and thus reduce formation of glycerol as a byproduct (Bakker et al., 2001), further research is needed to improve anaerobic nitrate reduction by engineered strains.

The ability of the spoilage yeast *B. bruxellensis* to assimilate nitrate is frequently cited as explanation for contamination *S. cerevisiae* sugarcane juice fermentations (da Silva et al., 2016; de Barros Pita et al., 2011). Our experiments with laboratory co-cultures demonstrate that, indeed, engineering of nitrate assimilation into *S. cerevisiae* can positively influence competition with *B. bruxellensis*. However, despite a slightly higher growth rate on nitrate of the engineered *S. cerevisiae* strain as compared to *B. bruxellensis* CBS 2499 (0.14 ± 0.01 h^{-1} versus 0.10 ± 0.01 h^{-1}), it was eventually still outcompeted by the spoilage yeast. Although there is a small difference in growth rates when only nitrate is provided, it is worth noticing that the similar evolved isolate IMS817 grew with a growth rate of 0.30 ± 0.01 in SMD_{AN} where both ammoninum and nitrate were present. This value is much higher than what reported for *B. bruxellensis* in a similar medium (0.077 ± 0.004 h^{-1}) (Galafassi et al., 2013) and indicates that a nitrate assimilating *S. cerevisiae* strain may persist even longer in a co-culture experiment where a media with both nitrogen sources is used. It was previously reported that dominance of *B. bruxellensis* seems not only related to its ability to assimilate nitrate but also to its higher affinity glucose importers (Blomqvist et al., 2012; Tiukova et al., 2019). This suggests that additional engineering is required to further increase *S. cerevisiae* competitiveness.

Further optimization of the kinetics of nitrate uptake and assimilation under the anaerobic conditions prevalent in industrial bioethanol production, combined with growth experiments on industrial media, are required to assess the full potential of this approach.

Author contributions

TP JTP and JMD designed the experiments and wrote a first version of the manuscript. All authors critically read this version, provided input and approved the final version. MW and TP constructed the *O. parapolymorpha* strains and performed the spot plate assay. TP constructed the *S. cerevisiae* strains and performed strain characterization in shake flasks and *in vitro*. MvdB and TP analysed the genome sequence data. DNAvdV and TP performed the competition experiment and prepared the proteomics samples.

Declaration of competing interest

The authors declare the following financial interests/personal relationships which may be considered as potential competing interests: Thomas Perli, Jack T Pronk and Jean-Marc G Daran are inventors on a patent application related to this work (WO2020209718 (A1) - 2020-10-15) Yeast with engineered molybdenum co-factor biosynthesis). The remaining authors have no competing interests to declare.

Acknowledgments

We thank Maxime den Ridder and Dr. Martin Pabst for helping us with the proteomics sample preparation and Dr. Irina Borodina and Dr. Tune Wulff for helping us with the proteomics sample analysis. This work was supported by the European Union's Horizon 2020 Research and Innovation Programme under the Marie Skłodowska-Curie action PAcMEN (grant agreement No 722287). JTP. acknowledges support by an Advanced Grant of the European Research Council (grant # 694633). TP, JTP and J-MGD. are inventors on a patent application related to this work (WO2020209718 – Yeast with engineered molybdenum co-factor biosynthesis). The remaining authors have no competing interests to declare.

Appendix A. Supplementary data

Supplementary data to this article can be found online at https://doi.org/10.1016/j.ymben.2021.02.004.

References

Abbott, D.A., Hynes, S.H., Ingledew, W.M., 2005. Growth rates of *Dekkera/Brettanomyces* yeasts hinder their ability to compete with *Saccharomyces cerevisiae* in batch corn mash fermentations. Appl. Microbiol. Biotechnol. 66, 641–647.

Alberts, B., 2018. Molecular Biology of the Cell.

Altschul, S.F., Gish, W., Miller, W., Myers, E.W., Lipman, D.J., 1990. Basic local alignment search tool. J. Mol. Biol. 215, 403–410.

Bakker, B.M., Overkamp, K.M., van Maris, A.J., Kötter, P., Luttik, M.A., van Dijken, J.P., Pronk, J.T., 2001. Stoichiometry and compartmentation of NADH metabolism in *Saccharomyces cerevisiae*. FEMS Microbiol. Rev. 25, 15–37.

Blomqvist, J., Nogue, V.S., Gorwa-Grauslund, M., Passoth, V., 2012. Physiological requirements for growth and competitiveness of *Dekkera bruxellensis* under oxygen-limited or anaerobic conditions. Yeast 29, 265–274.

Boonekamp, F.J., Dashko, S., Duiker, D., Gehrmann, T., van den Broek, M., den Ridder, M., Pabst, M., Robert, V., Abeel, T., Postma, E.D., Daran, J.M., Daran-Lapujade, P., 2020. Design and experimental evaluation of a minimal, innocuous watermarking strategy to distinguish near-Identical DNA and RNA sequences. ACS Synth. Biol. 9, 1361–1375.

Boonekamp, F.J., Dashko, S., van den Broek, M., Gehrmann, T., Daran, J.M., Daran-Lapujade, P., 2018. The genetic makeup and expression of the glycolytic and fermentative pathways are highly conserved within the *Saccharomyces* genus. Front. Genet. 9, 504.

Bracher, J.M., de Hulster, E., Koster, C.C., van den Broek, M., Daran, J.G., van Maris, A.J. A., Pronk, J.T., 2017. Laboratory evolution of a biotin-requiring *Saccharomyces cerevisiae* strain for full biotin prototrophy and identification of causal mutations. Appl. Environ. Microbiol. 83.

Broderick, J.B., 2001. Coenzymes and Cofactors. eLS.

Burkholder, P.R., McVeigh, I., Moyer, D., 1944. Studies on some growth factors of yeasts. J. Bacteriol. 48, 385–391.

Camadro, J.M., Thome, F., Brouillet, N., Labbe, P., 1994. Purification and properties of protoporphyrinogen oxidase from the yeast *Saccharomyces cerevisiae*. Mitochondrial location and evidence for a precursor form of the protein. J. Biol. Chem. 269, 32085–32091.

Campbell, W.H., 1999. Nitrate reductase structure, function and regulation: bridging the gap between biochemistry and physiology. Annu. Rev. Plant Physiol. Plant Mol. Biol. 50, 277–303.

Champe, P.C., Harvey, R.A., Ferrier, D.R., 2005. Biochemistry. Lippincott Williams & Wilkins.

Combs Jr., G.F., McClung, J.P., 2016. The Vitamins: Fundamental Aspects in Nutrition and Health. Academic press.

Costello, C., Griffin, W.M., Landis, A.E., Matthews, H.S., 2009. Impact of biofuel crop production on the formation of hypoxia in the Gulf of Mexico. Environ. Sci. Technol. 43, 7985–7991.

Crauwels, S., Van Assche, A., de Jonge, R., Borneman, A.R., Verreth, C., Troels, P., De Samblanx, G., Marchal, K., Van de Peer, Y., Willems, K.A., Verstrepen, K.J., Curtin, C.D., Lievens, B., 2015. Comparative phenomics and targeted use of genomics reveals variation in carbon and nitrogen assimilation among different *Brettanomyces bruxellensis* strains. Appl. Microbiol. Biotechnol. 99, 9123–9134.

Cvetkovic, A., Menon, A.L., Thorgersen, M.P., Scott, J.W., Poole, F.L., Jenney Jr., F.E., Lancaster, W.A., Praissman, J.L., Shanmukh, S., Vaccaro, B.J., Trauger, S.A., Kalisiak, E., Apon, J.V., Siuzdak, G., Yannone, S.M., Tainer, J.A., Adams, M.W., 2010. Microbial metalloproteomes are largely uncharacterized. Nature 466, 779–782.

da Silva, T.C., Leite, F.C., De Morais Jr., M.A., 2016. Distribution of *Dekkera bruxellensis* in a sugarcane-based fuel ethanol fermentation plant. Lett. Appl. Microbiol. 62, 354–358.

de Barros Pita, W., Leite, F.C., de Souza Liberal, A.T., Simoes, D.A., de Morais Jr., M.A., 2011. The ability to use nitrate confers advantage to *Dekkera bruxellensis* over *S. cerevisiae* and can explain its adaptation to industrial fermentation processes. Antonie Leeuwenhoek 100, 99–107.

de Barros Pita, W., Tiukova, I., Leite, F.C., Passoth, V., Simoes, D.A., de Morais Jr., M.A., 2013. The influence of nitrate on the physiology of the yeast *Dekkera bruxellensis* grown under oxygen limitation. Yeast 30, 111–117.

de Souza Liberal, A.T., Basilio, A.C., do Monte Resende, A., Brasileiro, B.T., da Silva-Filho, E.A., de Morais, J.O., Simoes, D.A., de Morais Jr., M.A., 2007. Identification of *Dekkera bruxellensis* as a major contaminant yeast in continuous fuel ethanol fermentation. J. Appl. Microbiol. 102, 538–547.

Dekker, W.J.C., Wiersma, S.J., Bouwknegt, J., Mooiman, C., Pronk, J.T., 2019. Anaerobic growth of *Saccharomyces cerevisiae* CEN.PK113-7D does not depend on synthesis or supplementation of unsaturated fatty acids. FEMS Yeast Res. 19.
Deves, R., Boyd, C.A., 1989. The determination of kinetic parameters for carrier-mediated transport of non-labelled substrate analogues: a general method applied to the study of divalent anion transport in placental membrane vesicles. Proc. R. Soc. Lond. B Biol. Sci. 237, 85–97.
Engler, C., Kandzia, R., Marillonnet, S., 2008. A one pot, one step, precision cloning method with high throughput capability. PloS One 3, e3647.
Entian, K.D., Kötter, P., 2007. Yeast genetic strain and plasmid collections. Methods Microbiol. 36, 629–666.
Facklam, T.J., Marzluf, G.A., 1978. Nitrogen regulation of amino acid catabolism in *Neurospora crassa*. Biochem. Genet. 16, 343–354.
Fitzpatrick, K.L., Tyerman, S.D., Kaiser, B.N., 2008. Molybdate transport through the plant sulfate transporter SHST1. FEBS Lett. 582, 1508–1513.
Galafassi, S., Capusoni, C., Moktaduzzaman, M., Compagno, C., 2013. Utilization of nitrate abolishes the "Custers effect" in *Dekkera bruxellensis* and determines a different pattern of fermentation products. J. Ind. Microbiol. Biotechnol. 40, 297–303.
Galanie, S., Thodey, K., Trenchard, I.J., Filsinger Interrante, M., Smolke, C.D., 2015. Complete biosynthesis of opioids in yeast. Science 349, 1095–1100.
Giaever, G., Chu, A.M., Ni, L., Connelly, C., Riles, L., Veronneau, S., Dow, S., Lucau-Danila, A., Anderson, K., Andre, B., Arkin, A.P., Astromoff, A., El-Bakkoury, M., Bangham, R., Benito, R., Brachat, S., Campanaro, S., Curtiss, M., Davis, K., Deutschbauer, A., Entian, K.D., Flaherty, P., Foury, F., Garfinkel, D.J., Gerstein, M., Gotte, D., Guldener, U., Hegemann, J.H., Hempel, S., Herman, Z., Jaramillo, D.F., Kelly, D.E., Kelly, S.L., Kötter, P., LaBonte, D., Lamb, D.C., Lan, N., Liang, H., Liao, H., Liu, L., Luo, C., Lussier, M., Mao, R., Menard, P., Ooi, S.L., Revuelta, J.L., Roberts, C.J., Rose, M., Ross-Macdonald, P., Scherens, B., Schimmack, G., Shafer, B., Shoemaker, D.D., Sookhai-Mahadeo, S., Storms, R.K., Strathern, J.N., Valle, G., Voet, M., Volckaert, G., Wang, C.Y., Ward, T.R., Wilhelmy, J., Winzeler, E.A., Yang, Y., Yen, G., Youngman, E., Yu, K., Bussey, H., Boeke, J.D., Snyder, M., Philippsen, P., Davis, R.W., Johnston, M., 2002. Functional profiling of the *Saccharomyces cerevisiae* genome. Nature 418, 387–391.
Gibson, D.G., Young, L., Chuang, R.Y., Venter, J.C., Hutchison 3rd, C.A., Smith, H.O., 2009. Enzymatic assembly of DNA molecules up to several hundred kilobases. Nat. Methods 6, 343–345.
Gietz, R.D., Woods, R.A., 2002. Transformation of yeast by lithium acetate/single-stranded carrier DNA/polyethylene glycol method. Methods Enzymol. 350, 87–96.
Gorter de Vries, A.R., de Groot, P.A., van den Broek, M., Daran, J.G., 2017. CRISPR-Cas9 mediated gene deletions in lager yeast *Saccharomyces pastorianus*. Microb. Cell Factories 16, 222.
Guerrero, M.G., Vega, J.M., Losada, M., 1981. The assimilatory nitrate-reducing system and its regulation. Annu. Rev. Plant Physiol. 32, 169–204.
Hille, R., 2002. Molybdenum and tungsten in biology. Trends Biochem. Sci. 27, 360–367.
Hille, R., Hall, J., Basu, P., 2014. The mononuclear molybdenum enzymes. Chem. Rev. 114, 3963–4038.
Inoue, H., Nojima, H., Okayama, H., 1990. High efficiency transformation of *Escherichia coli* with plasmids. Gene 96, 23–28.
Iobbi-Nivol, C., Leimkuhler, S., 2013. Molybdenum enzymes, their maturation and molybdenum cofactor biosynthesis in *Escherichia coli*. Biochim. Biophys. Acta 1827, 1086–1101.
Jespersen, L., Jakobsen, M., 1996. Specific spoilage organisms in breweries and laboratory media for their detection. Int. J. Food Microbiol. 33, 139–155.
Juergens, H., Varela, J.A., de Vries, A.R.G., Perli, T., Gast, V.J.M., Gyurchev, N.Y., Rajkumar, A.S., Mans, R., Pronk, J.T., Morrissey, J.P., Daran, J.M.G., 2018. Genome editing in *Kluyveromyces* and *Ogataea* yeasts using a broad-host-range Cas9/gRNA co-expression plasmid. FEMS Yeast Res. 18.
Kispal, G., Csere, P., Guiard, B., Lill, R., 1997. The ABC transporter Atm1p is required for mitochondrial iron homeostasis. FEBS Lett. 418, 346–350.
Kispal, G., Csere, P., Prohl, C., Lill, R., 1999. The mitochondrial proteins Atm1p and Nfs1p are essential for biogenesis of cytosolic Fe/S proteins. EMBO J. 18, 3981–3989.
Kuijpers, N.G., Solis-Escalante, D., Luttik, M.A., Bisschops, M.M., Boonekamp, F.J., van den Broek, M., Pronk, J.T., Daran, J.M., Daran-Lapujade, P., 2016. Pathway swapping: toward modular engineering of essential cellular processes. Proc. Natl. Acad. Sci. U. S. A. 113, 15060–15065.
Lake, M.W., Temple, C.A., Rajagopalan, K.V., Schindelin, H., 2000. The crystal structure of the *Escherichia coli* MobA protein provides insight into molybdopterin guanine dinucleotide biosynthesis. J. Biol. Chem. 275, 40211–40217.
Lee, M.E., DeLoache, W.C., Cervantes, B., Dueber, J.E., 2015. A highly characterized yeast toolkit for modular, multipart assembly. ACS Synth. Biol. 4, 975–986.
Leighton, J., Schatz, G., 1995. An ABC transporter in the mitochondrial inner membrane is required for normal growth of yeast. EMBO J. 14, 188–195.
Leimkuhler, S., Buhning, M., Beilschmidt, L., 2017. Shared sulfur mobilization routes for tRNA thiolation and molybdenum cofactor biosynthesis in prokaryotes and eukaryotes. Biomolecules 7.
Leimkuhler, S., Iobbi-Nivol, C., 2016. Bacterial molybdoenzymes: old enzymes for new purposes. FEMS Microbiol. Rev. 40, 1–18.
Li, Y., Smolke, C.D., 2016. Engineering biosynthesis of the anticancer alkaloid noscapine in yeast. Nat. Commun. 7, 12137.
Linder, T., 2019. A genomic survey of nitrogen assimilation pathways in budding yeasts (sub-phylum Saccharomycotina). Yeast 36, 259–273.
Llamas, A., Mendel, R.R., Schwarz, G., 2004. Synthesis of adenylated molybdopterin: an essential step for molybdenum insertion. J. Biol. Chem. 279, 55241–55246.
Llamas, A., Otte, T., Multhaup, G., Mendel, R.R., Swcharz, G., 2006. The mechanism of nucleotide-assisted molybdenum insertion into molybdopterin. A novel route toward metal cofactor assembly. J. Biol. Chem. 281 (27), 18343–18350. https://doi.org/10.1074/jbc.M601415200. Epub 2006 Apr 24.
Looke, M., Kristjuhan, K., Kristjuhan, A., 2011. Extraction of genomic DNA from yeasts for PCR-based applications. Biotechniques 50, 325. -+.
Madeira, F., Park, Y.M., Lee, J., Buso, N., Gur, T., Madhusoodanan, N., Basutkar, P., Tivey, A.R.N., Potter, S.C., Finn, R.D., Lopez, R., 2019. The EMBL-EBI search and sequence analysis tools APIs in 2019. Nucleic Acids Res. 47, W636–W641.
Maia, L.B., Moura, J.J., Moura, I., 2015. Molybdenum and tungsten-dependent formate dehydrogenases. J. Biol. Inorg. Chem. 20, 287–309.
Mans, R., van Rossum, H.M., Wijsman, M., Backx, A., Kuijpers, N.G.A., van den Broek, M., Daran-Lapujade, P., Pronk, J.T., van Maris, A.J.A., Daran, J.M.G., 2015. CRISPR/Cas9: a molecular Swiss army knife for simultaneous introduction of multiple genetic modifications in *Saccharomyces cerevisiae*. FEMS Yeast Res. 15.
Marelja, Z., Mullick Chowdhury, M., Dosche, C., Hille, C., Baumann, O., Lohmannsroben, H.G., Leimkuhler, S., 2013. The L-cysteine desulfurase NFS1 is localized in the cytosol where it provides the sulfur for molybdenum cofactor biosynthesis in humans. PloS One 8, e60869.
Marelja, Z., Stocklein, W., Nimtz, M., Leimkuhler, S., 2008. A novel role for human Nfs1 in the cytoplasm: Nfs1 acts as a sulfur donor for MOCS3, a protein involved in molybdenum cofactor biosynthesis. J. Biol. Chem. 283, 25178–25185.
Mendel, R.R., 2013. The molybdenum cofactor. J. Biol. Chem. 288, 13165–13172.
Milne, N., Luttik, M.A.H., Cueto Rojas, H.F., Wahl, A., van Maris, A.J.A., Pronk, J.T., Daran, J.M., 2015. Functional expression of a heterologous nickel-dependent, ATP-independent urease in *Saccharomyces cerevisiae*. Metab. Eng. 30, 130–140.
Nielsen, J., 2019. Yeast systems biology: model organism and cell factory. Biotechnol. J. 14, e1800421.
Nijkamp, J.F., van den Broek, M.A., Geertman, J.M., Reinders, M.J., Daran, J.M., de Ridder, D., 2012. *De novo* detection of copy number variation by co-assembly. Bioinformatics 28, 3195–3202.
Ostergaard, S., Olsson, L., Nielsen, J., 2000. Metabolic engineering of *Saccharomyces cerevisiae*. Microbiol. Mol. Biol. Rev. 64, 34–50.
Palmer, T., Santini, C.L., Iobbi-Nivol, C., Eaves, D.J., Boxer, D.H., Giordano, G., 1996. Involvement of the narJ and mob gene products in distinct steps in the biosynthesis of the molybdoenzyme nitrate reductase in *Escherichia coli*. Mol. Microbiol. 20, 875–884.
Parente, D.C., Cajueiro, D.B.B., Moreno, I.C.P., Leite, F.C.B., Pita, W.D., De Morais, M.A., 2018. On the catabolism of amino acids in the yeast *Dekkera bruxellensis* and the implications for industrial fermentation processes. Yeast 35, 299–309.
Pena-Moreno, I.C., Castro Parente, D., da Silva, J.M., Andrade Mendonca, A., Rojas, L.A. V., de Morais Junior, M.A., de Barros Pita, W., 2019. Nitrate boosts anaerobic ethanol production in an acetate-dependent manner in the yeast *Dekkera bruxellensis*. J. Ind. Microbiol. Biotechnol. 46, 209–220.
Peng, T., Xu, Y., Zhang, Y., 2018. Comparative genomics of molybdenum utilization in prokaryotes and eukaryotes. BMC Genom. 19, 691.
Perli, T., Moonen, D.P.I., van den Broek, M., Pronk, J.T., Daran, J.M., 2020a. Adaptive laboratory evolution and reverse engineering of single-vitamin prototrophies in *Saccharomyces cerevisiae*. Appl. Environ. Microbiol. 86.
Perli, T., Vos, A.M., Bouwknegt, J., Dekker, W.J.C., Wiersma, S.J., Mooiman, C., Ortiz-Merino, R.A., Daran, J.-M., Pronk, J.T., 2020b. Identification of oxygen-independent pathways for pyridine-nucleotide and Coenzyme-A synthesis in anaerobic fungi by expression of candidate genes in yeast. bioRxiv, 2020.07.06.189415.
Perli, T., Wronska, A.K., Ortiz-Merino, R.A., Pronk, J.T., Daran, J.M., 2020c. Vitamin requirements and biosynthesis in *Saccharomyces cerevisiae*. Yeast 37, 283–304.
Phalip, V., Kuhn, I., Lemoine, Y., Jeltsch, J.M., 1999. Characterization of the biotin biosynthesis pathway in *Saccharomyces cerevisiae* and evidence for a cluster containing *BIO5*, a novel gene involved in vitamer uptake. Gene 232, 43–51.
Protchenko, O., Shakoury-Elizeh, M., Keane, P., Storey, J., Androphy, R., Philpott, C.C., 2008. Role of *PUG1* in inducible porphyrin and heme transport in *Saccharomyces cerevisiae*. Eukaryot. Cell 7, 859–871.
Rajagopalan, K.V., Johnson, J.L., 1992. The pterin molybdenum cofactors. J. Biol. Chem. 267, 10199–10202.
Ravin, N.V., Eldarov, M.A., Kadnikov, V.V., Beletsky, A.V., Schneider, J., Mardanova, E. S., Smekalova, E.M., Zvereva, M.I., Dontsova, O.A., Mardanov, A.V., Skryabin, K.G., 2013. Genome sequence and analysis of methylotrophic yeast *Hansenula polymorpha* DL1. BMC Genom. 14, 837.
Raymond, C.K., Pownder, T.A., Sexson, S.L., 1999. General method for plasmid construction using homologous recombination. Biotechniques 26 (134–8), 140–141.
Reschke, S., Duffus, B.R., Schrapers, P., Mebs, S., Teutloff, C., Dau, H., Haumann, M., Leimkuhler, S., 2019. Identification of YdhV as the first molybdoenzyme binding a Bis-Mo-MPT cofactor in *Escherichia coli*. Biochemistry 58, 2228–2242.
Rubio, L.M., Ludden, P.W., 2008. Biosynthesis of the iron-molybdenum cofactor of nitrogenase. Annu. Rev. Microbiol. 62, 93–111.
Salazar, A.N., de Vries, A.R.G., van den Broek, M., Wijsman, M., Cortes, P.D., Brickwedde, A., Brouwers, N., Daran, J.M.G., Abeel, T., 2017. Nanopore sequencing enables near-complete *de novo* assembly of *Saccharomyces cerevisiae* reference strain CEN.PK113-7D. FEMS Yeast Res. 17.
Saraya, R., Gidijala, L., Veenhuis, M., van der Klei, I.J., 2014. Tools for genetic engineering of the yeast *Hansenula polymorpha*. Methods Mol. Biol. 1152, 43–62.
Schaedler, T.A., Thornton, J.D., Kruse, I., Schwarzlander, M., Meyer, A.J., van Veen, H. W., Balk, J., 2014. A conserved mitochondrial ATP-binding cassette transporter exports glutathione polysulfide for cytosolic metal cofactor assembly. J. Biol. Chem. 289, 23264–23274.
Schwarz, G., Mendel, R.R., Ribbe, M.W., 2009. Molybdenum cofactors, enzymes and pathways. Nature 460, 839–847.

Shen, X.X., Opulente, D.A., Kominek, J., Zhou, X., Steenwyk, J.L., Buh, K.V., Haase, M.A. B., Wisecaver, J.H., Wang, M., Doering, D.T., Boudouris, J.T., Schneider, R.M., Langdon, Q.K., Ohkuma, M., Endoh, R., Takashima, M., Manabe, R.I., Cadez, N., Libkind, D., Rosa, C.A., DeVirgilio, J., Hulfachor, A.B., Groenewald, M., Kurtzman, C.P., Hittinger, C.T., Rokas, A., 2018. Tempo and mode of genome evolution in the budding yeast subphylum. Cell 175, 1533–1545 e20.

Siverio, J.M., 2002. Assimilation of nitrate by yeasts. FEMS Microbiol. Rev. 26, 277–284.

Smith, M.T., Yamazaki, M., Poot, G.A., 1990. *Dekkera, Brettanomyces* and *Eeniella*: electrophoretic comparison of enzymes and DNA-DNA homology. Yeast 6, 299–310.

Solis-Escalante, D., Kuijpers, N.G., Bongaerts, N., Bolat, I., Bosman, L., Pronk, J.T., Daran, J.M., Daran-Lapujade, P., 2013. amdSYM, a new dominant recyclable marker cassette for *Saccharomyces cerevisiae*. FEMS Yeast Res. 13, 126–139.

Stolz, J., Hoja, U., Meier, S., Sauer, N., Schweizer, E., 1999. Identification of the plasma membrane H+-biotin symporter of *Saccharomyces cerevisiae* by rescue of a fatty acid-auxotrophic mutant. J. Biol. Chem. 274, 18741–18746.

Suh, S.O., Zhou, J.L.J., 2010. Methylotrophic yeasts near *Ogataea* (*Hansenula) polymorpha*: a proposal of *Ogataea angusta* comb. nov and *Candida parapolymorpha* sp nov. FEMS Yeast Res. 10, 631–638.

Tejada-Jimenez, M., Llamas, A., Sanz-Luque, E., Galvan, A., Fernandez, E., 2007. A high-affinity molybdate transporter in eukaryotes. Proc. Natl. Acad. Sci. U. S. A. 104, 20126–20130.

Teschner, J., Lachmann, N., Schulze, J., Geisler, M., Selbach, K., Santamaria-Araujo, J., Balk, J., Mendel, R.R., Bittner, F., 2010. A novel role for *Arabidopsis* mitochondrial ABC transporter ATM3 in molybdenum cofactor biosynthesis. Plant Cell 22, 468–480.

Tiukova, I.A., Moller-Hansen, I., Belew, Z.M., Darbani, B., Boles, E., Nour-Eldin, H.H., Linder, T., Nielsen, J., Borodina, I., 2019. Identification and characterisation of two high-affinity glucose transporters from the spoilage yeast *Brettanomyces bruxellensis*. FEMS Microbiol. Lett. 366.

Truong, H.N., Meyer, C., Daniel-Vedele, F., 1991. Characteristics of *Nicotiana tabacum* nitrate reductase protein produced in *Saccharomyces cerevisiae*. Biochem. J. 278 (Pt 2), 393–397.

van Rossum, H.M., Kozak, B.U., Niemeijer, M.S., Duine, H.J., Luttik, M.A.H., Boer, V.M., Kötter, P., Daran, J.M.G., van Maris, A.J.A., Pronk, J.T., 2016. Alternative reactions at the interface of glycolysis and citric acid cycle in *Saccharomyces cerevisiae*. FEMS Yeast Res. 16.

Verduyn, C., Postma, E., Scheffers, W.A., Van Dijken, J.P., 1992. Effect of benzoic acid on metabolic fluxes in yeasts: a continuous-culture study on the regulation of respiration and alcoholic fermentation. Yeast 8, 501–517.

Verhoeven, M.D., Lee, M., Kamoen, L., van den Broek, M., Janssen, D.B., Daran, J.M.G., van Maris, A.J.A., Pronk, J.T., 2017. Mutations in *PMR1* stimulate xylose isomerase activity and anaerobic growth on xylose of engineered *Saccharomyces cerevisiae* by influencing manganese homeostasis. Sci Rep-Uk 7.

Wierckx, N., Koopman, F., Ruijssenaars, H.J., de Winde, J.H., 2011. Microbial degradation of furanic compounds: biochemistry, genetics, and impact. Appl. Microbiol. Biotechnol. 92, 1095–1105.

Winzeler, E.A., Richards, D.R., Conway, A.R., Goldstein, A.L., Kalman, S., McCullough, M.J., McCusker, J.H., Stevens, D.A., Wodicka, L., Lockhart, D.J., Davis, R.W., 1998. Direct allelic variation scanning of the yeast genome. Science 281, 1194–1197.

Wronska, A.K., Haak, M.P., Geraats, E., Bruins Slot, E., van den Broek, M., Pronk, J.T., Daran, J.M., 2020. Exploiting the diversity of Saccharomycotina yeasts to engineer biotin-independent growth of *Saccharomyces cerevisiae*. Appl. Environ. Microbiol.

Wu, H., Ito, K., Shimoi, H., 2005. Identification and characterization of a novel biotin biosynthesis gene in *Saccharomyces cerevisiae*. Appl. Environ. Microbiol. 71, 6845–6855.

Zagorec, M., Buhler, J.M., Treich, I., Keng, T., Guarente, L., Labbe-Bois, R., 1988. Isolation, sequence, and regulation by oxygen of the yeast *HEM13* gene coding for coproporphyrinogen oxidase. J. Biol. Chem. 263, 9718–9724.

Zhang, Y., Rump, S., Gladyshev, V.N., 2011. Comparative genomics and evolution of Molybdenum utilization. Coord. Chem. Rev. 255, 1206–1217.